The Plant Cell, Vol. 26: 712–728, February 2014, www.plantcell.org

Targeted Degradation of Abscisic Acid Receptors Is Mediated by the Ubiquitin Ligase Substrate Adaptor DDA1 in *Arabidopsis*[W]

María Luisa Irigoyen,[a,1] Elisa Iniesto,[a,1] Lesia Rodriguez,[b] María Isabel Puga,[a] Yuki Yanagawa,[c,2] Elah Pick,[c,3] Elizabeth Strickland,[c,4] Javier Paz-Ares,[a] Ning Wei,[c] Geert De Jaeger,[d,e] Pedro L. Rodriguez,[b] Xing Wang Deng,[c] and Vicente Rubio[a,5]

[a] Centro Nacional de Biotecnología–Consejo Superior de Investigaciones Científicas, 28049 Madrid, Spain
[b] Instituto de Biología Molecular y Celular de Plantas, Consejo Superior de Investigaciones Científicas–Universidad Politécnica de Valencia, 46022 Valencia, Spain
[c] Department of Molecular, Cellular, and Developmental Biology, Yale University, New Haven, Connecticut 06520
[d] Department of Plant Systems Biology, VIB, B-9052 Ghent, Belgium
[e] Department of Plant Biotechnology and Bioinformatics, Ghent University, B-9052 Ghent, Belgium

ORCID ID: 0000-0002-8800-2400 (V.R.)

CULLIN4-RING E3 ubiquitin ligases (CRL4s) regulate key developmental and stress responses in eukaryotes. Studies in both animals and plants have led to the identification of many CRL4 targets as well as specific regulatory mechanisms that modulate their function. The latter involve COP10-DET1-DDB1 (CDD)–related complexes, which have been proposed to facilitate target recognition by CRL4, although the molecular basis for this activity remains largely unknown. Here, we provide evidence that *Arabidopsis thaliana* DET1-, DDB1-ASSOCIATED1 (DDA1), as part of the CDD complex, provides substrate specificity for CRL4 by interacting with ubiquitination targets. Thus, we show that DDA1 binds to the abscisic acid (ABA) receptor PYL8, as well as PYL4 and PYL9, in vivo and facilitates its proteasomal degradation. Accordingly, we found that DDA1 negatively regulates ABA-mediated developmental responses, including inhibition of seed germination, seedling establishment, and root growth. All other CDD components displayed a similar regulatory function, although they did not directly interact with PYL8. Interestingly, DDA1-mediated destabilization of PYL8 is counteracted by ABA, which protects PYL8 by limiting its polyubiquitination. Altogether, our data establish a function for DDA1 as a substrate receptor for CRL4-CDD complexes and uncover a mechanism for the desensitization of ABA signaling based on the regulation of ABA receptor stability.

INTRODUCTION

The regulation of protein function by posttranslational modification with ubiquitin (Ub) plays a fundamental role in many biological processes in eukaryotes. Ub conjugation to proteins (i.e., ubiquitination) may trigger proteasomal degradation of protein targets or changes in their properties (e.g., protein activity, localization, assembly, and interaction ability), depending on specific Ub chain configurations (Hershko and Ciechanover, 1998; Ikeda and Dikic, 2008; Deshaies and Joazeiro, 2009). Ubiquitination is mediated by an enzymatic cascade in which E3 Ub ligases (E3) provide the substrate specificity, with CULLIN RING ligases (CRLs) being the largest class of E3s. CRLs represent a family of modular complexes, consisting of at least seven different CULLIN scaffold proteins, each of them serving as a building block for the assembly of dozens or more multiple-subunit CRLs (Deshaies and Joazeiro, 2009). Among this class, CRL4 regulates key aspects of cell biology in eukaryotes, including cell cycle progression and DNA damage repair and replication (Jackson and Xiong, 2009; Biedermann and Hellmann, 2011). In plants, CRL4 functional significance can be realized by the number and relevance of the processes they regulate, which span the plant's whole life, including embryogenesis, seedling photomorphogenesis, circadian clock function, and flowering (Yu et al., 2008; Biedermann and Hellmann, 2011). As well, CRL4s regulate different abiotic stress responses, such as drought tolerance, nutrient deprivation, and DNA damage responses (Guo et al., 2013). Thus, several CRL4 protein targets have been identified in plants, including positive regulators of light signaling, flowering, metabolic homeostasis, DNA damage repair, and responses to the stress hormone abscisic acid (ABA) (reviewed in Biedermann and Hellmann, 2011; Guo et al., 2013). ABA has a central role in the regulation of seed germination and responses to abiotic stresses, such as drought, high salinity, and low temperatures (Chinnusamy et al., 2008; Hirayama and Shinozaki, 2010; Hauser et al., 2011). ABA signaling is mediated by the pyrabactin resistance/pyrabactin resistance–like/regulatory components of ABA receptor (PYR/PYL/RCAR) family of ABA receptors, which allows direct

[1] These authors contributed equally to this work.
[2] Current address: Plant-Microbe Interactions Research Unit, National Institute of Agrobiological Sciences, 2-1-2 Kannondai, Tsukuba, Ibaraki 305-8602, Japan.
[3] Current address: Department of Biology and Environment, Faculty of Natural Sciences, University of Haifa at Oranim, Tivon 36006, Israel.
[4] Current address: Blackburnian Consulting, Morristown, NJ 07960.
[5] Address correspondence to vrubio@cnb.csic.es.
The author responsible for distribution of materials integral to the findings presented in this article in accordance with the policy described in the Instructions for Authors (www.plantcell.org) is: Vicente Rubio (vrubio@cnb.csic.es).
[W] Online version contains Web-only data.
www.plantcell.org/cgi/doi/10.1105/tpc.113.122234

ABA-dependent inhibition of clade A phosphatases type 2C (PP2Cs), such as ABA INSENSITIVE1 (ABI1), HYPERSENSITIVE TO ABA1 (HAB1) and HAB2, and PP2CA, which are key negative regulators of the pathway (Saez et al., 2006; Rubio et al., 2009). Inhibition of PP2Cs leads to the activation of SUCROSE NONFERMENTING1–related subfamily 2 kinases that, in turn, regulate the transcriptional response to ABA by phosphorylating specific protein targets, including transcription factors of the ABA-responsive element binding/ABRE binding factor (ABF) family (Cutler et al., 2010; Nakashima and Yamaguchi-Shinozaki, 2013).

CRL4 uses CULLIN4 (CUL4) as a scaffold protein for the rest of the complex, RING finger protein RBX1 for Ub conjugase (E2) recruitment, and DAMAGED-SPECIFIC DNA BINDING PROTEIN1 (DDB1) for interaction with substrate receptors, namely DCAFs (for DDB1- and CUL4-associated factors) that usually contain WDxR motifs and recognize specific targets for ubiquitination. In *Arabidopsis thaliana*, there are two genes encoding DDB1 proteins, *DDB1A* and *DDB1B*. Although their products are 91% identical, they have partially distinct functions and may interact with different DCAF subsets to mediate the ubiquitination of specific protein substrates in each case (Schroeder et al., 2002). In addition to being a constituent of CRL4, DDB1 proteins also interact with CONSTITUTIVE PHOTOMORPHOGENIC10 (COP10) and DEETIOLATED1 (DET1) to form a stable complex termed CDD in plants (Schroeder et al., 2002; Yanagawa et al., 2004), which cooperates with CRL4 in response to developmental and stress signals, for example to promote the degradation of the transcription factor LONG HYPOCOTYL5 and the DCAF protein DAMAGED-SPECIFIC DNA BINDING PROTEIN2 (DDB2) under dark conditions and upon DNA damage, respectively (Osterlund et al., 2000; Castells et al., 2010). The CDD complex was originally isolated from floral meristems of cauliflower (*Brassica oleracea*, a species related to *Arabidopsis*) using a biochemical purification procedure (Yanagawa et al., 2004). In this complex, DDB1 acts as the core adaptor and allows CDD–CRL4 interaction (Chen et al., 2006; Bernhardt et al., 2010). COP10 is an E2 Ub conjugase variant that lacks the catalytic Cys required for Ub binding prior to target ubiquitination (Suzuki et al., 2002). Therefore, COP10 has no E2 activity; instead, it can enhance the activity of other canonical E2s (Yanagawa et al., 2004; Lau and Deng, 2009). Finally, DET1 is a multifunctional protein with no recognizable domains that enables targeted degradation of specific regulatory proteins, likely by recruiting additional DCAF proteins (Lau and Deng, 2012). Interestingly, the CDD complex is conserved in humans, where it has been termed DDD-E2, since it contains, in addition to DDB1 and DET1, a canonical E2 Ub conjugase (highly homologous to the E2 Ub conjugase variant COP10) and a small protein with no obvious motifs called DET1-, DDB1-ASSOCIATED1 (DDA1) (Pick et al., 2007). DDA1 is conserved in higher eukaryotes, including the model plant *Arabidopsis*. Functional characterization of human DDA1 (hDDA1) showed that it likely acts as a positive regulator of CRL4s, although the molecular basis of this activity is unknown (Olma et al., 2009).

Despite the biological relevance of CDD/DDD-E2 complexes, the molecular mechanisms by which they facilitate CRL4 function remain unclear. In this study, we shed light on this issue by characterizing *Arabidopsis* DDA1, which we show associates with both the CDD complex and CUL4 and is able to interact with specific protein targets. In this regard, we found that DDA1 physically binds to members of the PYR/PYL/RCAR family of ABA receptors, including PYL4, PYL8, and PYL9. Moreover, we found that DDA1 promotes proteasomal degradation of PYL8. Therefore, DDA1, together with the other CDD components, acts as a negative regulator of ABA signaling. Interestingly, ABA treatment attenuates DDA1's effect on PYL8 degradation, suggesting that ABA not only activates PYL8 but also inhibits its degradation, leading to increased ABA signaling. We conclude that DDA1 mediates the recognition of specific targets of CRL4 as part of a substrate adaptor module that includes the CDD complex. Moreover, we unveil a regulatory mechanism to modulate ABA responses based on the regulation of ABA receptor stability.

RESULTS

DDA1 Is Present in Vascular Plants

Arabidopsis DDA1 was originally identified as an ortholog of hDDA1 (Pick et al., 2007). To investigate whether DDA1 is conserved across plant families, we searched for DDA1-related sequences in plant genomic databases (see Methods). We successfully retrieved DDA1 homologs from 49 different plant species and subspecies (Supplemental Figure 1). On average, 66% amino acid sequence identity was found between DDA1 homolog pairs. Phylogenetic analyses showed that DDA1 is conserved in vascular plants, including the pteridophyte *Selaginella moellendorffii*, and could not be found in algae or in the moss *Physcomitrella patens* (Supplemental Figure 2). In the case of angiosperms, DDA1 was present in both monocots and dicots. In plant diploid species, including *Arabidopsis*, *DDA1* was found as a single-copy gene, although in some cases (e.g., maize [*Zea mays*], soybean [*Glycine max*], and cotton [*Gossypium hirsutum*]), we found two *DDA1* gene copies.

DDA1 Is a Component of the CDD Complex in *Arabidopsis*

hDDA1 was found to be part of DDD-E2 complexes in human cells. However, evidence for DDA1 association to the CDD complex, the counterpart of DDD-E2 complexes in plants, was missing. To determine whether DDA1 copurifies with the CDD complex, we subjected the original gel filtration fractions, corresponding to the last step of CDD purification (Yanagawa et al., 2004), to SDS-PAGE followed by silver staining or immunoblotting using a specific antibody raised against recombinant His-tagged DDA1 (Figure 1A). No additional bands beyond those previously reported were detected by silver staining of the SDS-PAGE gel. However, DDA1 could be immunodetected in fractions corresponding to the CDD as three protein bands that had a lower molecular mass (10 kD) than expected for the 16-kD DDA1 protein, indicating that, although apparently partly degraded, DDA1 is present in purified CDD samples (Supplemental Figure 3).

To further confirm that DDA1 binds to the CDD complex, we isolated DDA1-associated proteins using tandem affinity purification (TAP) techniques. For this, C-terminal TAP-tagged DDA1 was expressed and purified from two *Arabidopsis* cell cultures. The identities of proteins that copurified with DDA1-TAP were determined using mass spectrometry analysis (Supplemental Table 1).

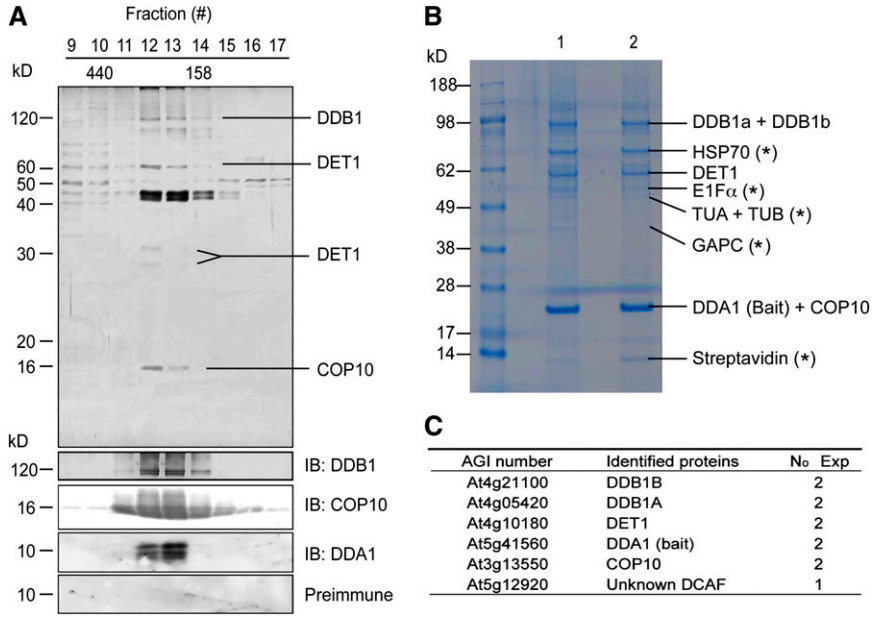

C

AGI number	Identified proteins	No. Exp
At4g21100	DDB1B	2
At4g05420	DDB1A	2
At4g10180	DET1	2
At5g41560	DDA1 (bait)	2
At3g13550	COP10	2
At5g12920	Unknown DCAF	1

Figure 1. DDA1 Associates with the CDD Complex in Planta.

(A) Gel filtration fractions obtained in the purification of the CDD complex from cauliflower were separated on a 15% SDS-PAGE gel and subjected to silver staining (top panel) or to immunoblot analysis (four other panels). Antibodies used in each case are shown on the right side. The positions of specific protein bands were determined according to data reported previously (Schroeder et al., 2002; Yanagawa et al., 2004).

(B) Isolation of DDA1-associated proteins by TAP techniques. DDA1-TAP fusion was expressed and purified from transgenic cell cultures in two experiments as indicated at the top. Protein bands obtained were excised, trypsin digested, and analyzed by mass spectrometry. Specific bands corresponding to bait and interactors are indicated. The DCAF protein band was not visible by Coomassie blue staining of the gel. Asterisks indicate the positions of experimental background proteins (see Methods).

(C) Specific proteins identified in **(B)** are listed. Arabidopsis Genome Initiative (AGI) loci identification numbers and names of proteins copurified with DDA1 are shown, together with the number of positive identifications in two independent TAP experiments.

Together with DDA1, TAP-purified samples contained all CDD complex components (Figures 1B and 1C). In this regard, DDA1 was incorporated into CDD complexes that contained either DDB1a or DDB1b, as both proteins copurified with DDA1-TAP. Next, we characterized DDA1 interaction with CDD complex components using yeast two-hybrid assays. In agreement with previous studies in mammalian systems (Jin et al., 2006; Pick et al., 2007; Olma et al., 2009), we found that DDA1 strongly binds to DDB1 proteins and that this interaction occurs through the β-propeller domain A (BPA) in DDB1 (Figure 2). The association of DDA1 into CDD complexes was likely mediated by the physical interaction of DDA1 and DDB1, since we did not observe direct binding of DDA1 to either DET1 or COP10. Upon DDA1-TAP purification, a DCAF protein (encoded by the At5g12920 locus) (Lee et al., 2008) was also copurified (Figures 1B and 1C). This DCAF protein interacted with DDB1a in yeast two-hybrid assays but not with DDA1, indicating that the DDA1-DCAF association is indirect and likely mediated by DDB1 proteins (Figure 2B).

DDA1 Associates in Vivo with CUL4

hDDA1, likely as part of DDD-E2 complexes, has been found to associate with CRL4 in mammalian cells (Olma et al., 2009). In order to test whether this is the case for *Arabidopsis* DDA1, we first generated *Arabidopsis* transgenic plants expressing the cDNA of DDA1 fused to green fluorescent protein (GFP) under the control of the cauliflower mosaic virus 35S promoter (oeDDA1-GFP). *DDA1-GFP* expression levels were analyzed in oeDDA1-GFP transgenic lines by quantitative RT-PCR (qRT-PCR) (Figure 3A). Independent lines tested displayed high levels of *DDA1-GFP* expression, ranging from 100- to 1000-fold the endogenous *DDA1* transcript level in wild-type plants. To test whether the resulting DDA1-GFP fusion is able to associate with the CDD complex, we crossed oeDDA1-GFP plants (line 3; Figure 3A) with a previously described 3xFLAG epitope–tagged COP10-expressing line (FLAG-COP10; Yanagawa et al., 2004) and conducted immunoprecipitation assays. As shown in Figure 3B, FLAG-COP10 coimmunoprecipitated with DDA1-GFP. Since DDA1 and COP10 do not directly interact, according to our yeast two-hybrid assays (Figure 2B), we concluded that DDA1-GFP and FLAG-COP10 were incorporated in the same CDD complexes. Moreover, CUL4 protein was detected in DDA1-GFP immunoprecipitates using specific anti-CUL4 antibodies (Figure 3C). Taken together, these results indicate that DDA1, likely as part of the CDD, interacts with CUL4-containing (i.e., CRL4) complexes.

DDA1 Physically Interacts with PYR/PYL/RCAR ABA Receptors

The molecular basis of DDA1 activity is unclear. To get insights into its mechanism of action, we searched for proteins that interact with DDA1. With this aim, we conducted a yeast two-hybrid screen

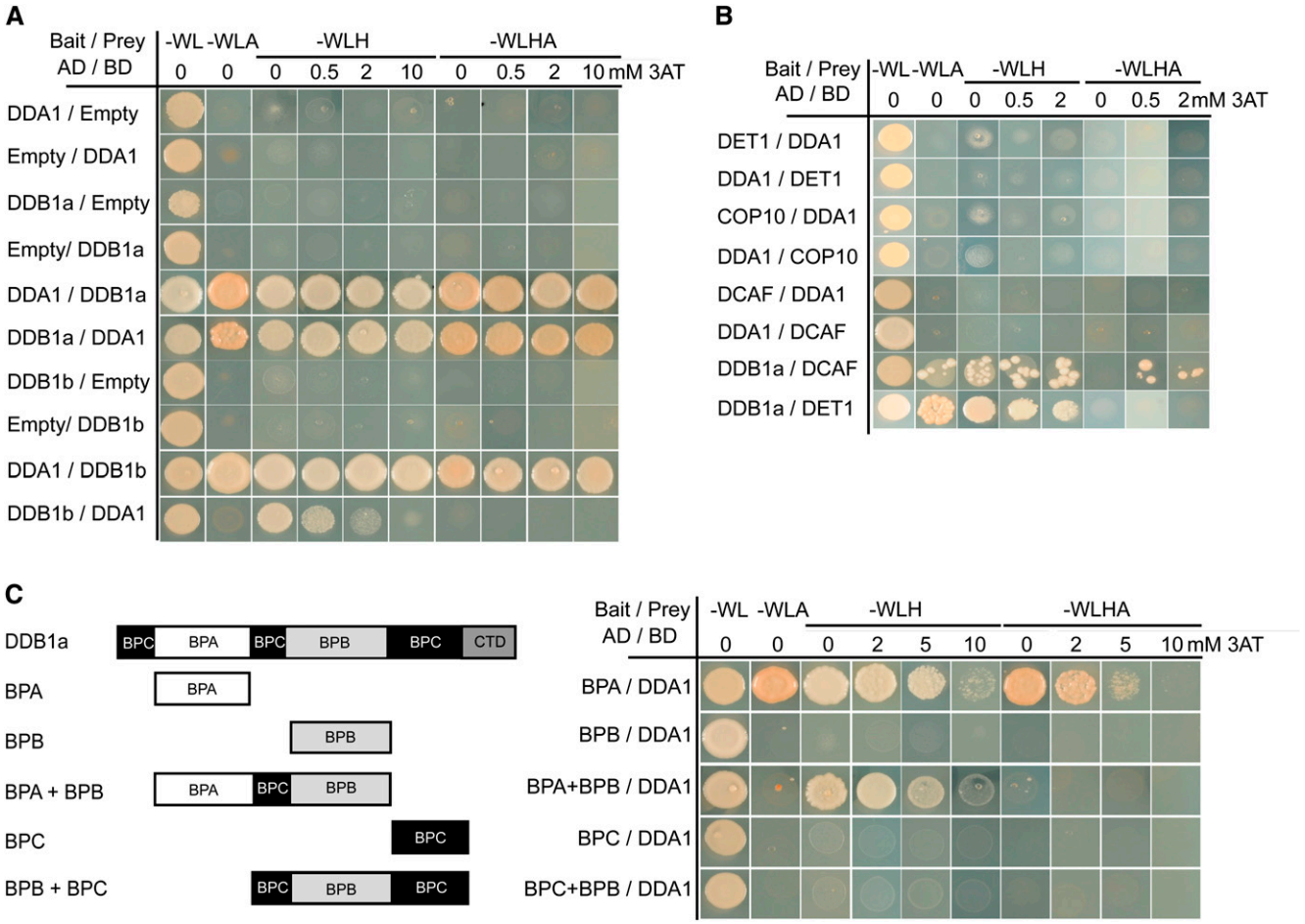

Figure 2. DDA1 Directly Binds to DDB1 Proteins.

(A) and **(B)** DDA1 interacts with DDB1 proteins in yeast two-hybrid assays. DDA1 interaction with CDD complex components DDB1a and DDB1b **(A)** and DET1, COP10, and a yet-to-be characterized DCAF protein **(B)** was assessed. The growth of yeast transformed with the indicated constructs on selective plates is shown. Selective media contained different concentrations of 3-amino-1,2,4-triazole (3AT; ranging from 0.5 to 10 mM). A previously reported DET1–DDB1a interaction was used as a positive control. Empty vectors were used as negative controls.

(C) DDA1 interacts with the BPA domain in DDB1a. Interaction of DDA1 with a series of DDB1a deletion constructs, containing different domain combinations (left panel), was assessed in yeast two-hybrid experiments (right panel). Experimental conditions were as in **(A)** and **(B)**.

using DDA1 as bait. The full-length coding sequence of DDA1 fused to the binding domain of GAL4 was used to screen a cDNA library prepared from *Arabidopsis* seedlings. From over 15 million clones screened, 200 were identified as potential DDA1 interactors. Among them, 20 were subsequently confirmed by retransformation into yeast. Interestingly, among the DDA1 interactors, we found two clones corresponding to truncated versions of the ABA receptors PYL4 (amino acids 84 to 207) and PYL9 (amino acids 75 to 187) (Figure 4A). We aimed to determine whether DDA1 interacts with other *Arabidopsis* PYR/PYL/RCAR family members using yeast two-hybrid assays. As a result, we found that DDA1 additionally binds to PYL8 (Figure 4B). Interestingly, PYL8 did not interact with other components of the CDD in these assays.

To confirm DDA1 interaction with PYL4, PYL8, and PYL9 in planta, we performed bimolecular fluorescence complementation (BiFC) assays. For this, *Nicotiana benthamiana* leaves were coinfiltrated with *Agrobacterium tumefaciens* cells to express DDA1 and full-length ABA receptor fusions with the N- or C-terminal portions of the yellow fluorescent protein (YFP). The infiltrated leaves were analyzed with the confocal fluorescence microscope 3 d after infiltration. Physical interaction between DDA1 and the three ABA receptors tested was revealed by reconstitution of YFP fluorescence in cells coinfiltrated with constructs corresponding to DDA1:YFPC and YFPN:PYL (PYL4, PYL8, or PYL9), whereas expression of DDA1 or receptor constructs alone did not restore the YFP fluorescence (Figure 4C; Supplemental Figure 4). Interaction between DDA1 and ABA receptors occurred in nuclei, since fluorescent signal resulting from their interaction colocalizes with 4′,6-diamidino-2-phenylindole (DAPI) staining (Figure 4C; Supplemental Figure 4B). To assess the confidence of such interactions, the percentage of YFP fluorescent nuclei was calculated using PYL8 as an ABA receptor

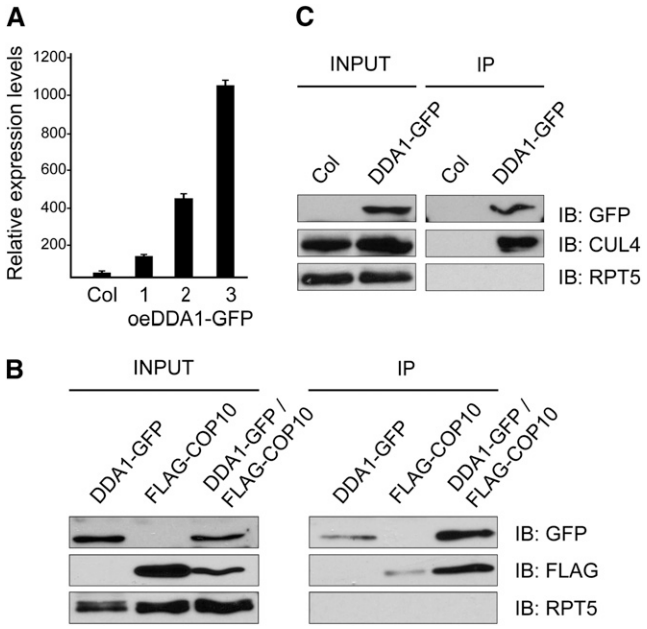

Figure 3. DDA1 Associates with CUL4 in Vivo.

(A) qRT-PCR analysis of DDA1-GFP expression levels in three independent oeDDA1-GFP lines compared with endogenous DDA1 in wild-type plants (Col). Data are means of three biological replicates with two technical replicates per sample. Error bars represent SD.

(B) DDA1-GFP associates with FLAG-COP10 in vivo. Immunoprecipitation of DDA1-GFP fusions was performed using total protein extracts prepared from 8-d-old oeDDA1-GFP, oeFLAG-COP10, and oeDDA1-GFP/oeFLAG-COP10 seedlings. Total extracts (INPUT) and immunoprecipitates (IP) were subjected to immunoblot analysis with anti-GFP and anti-FLAG antibodies to detect DDA1-GFP and FLAG-COP10, respectively. Immunoblots against RPT5 were used as a loading control.

(C) CUL4 coimmunoprecipitates with DDA1-GFP in vivo. Immunoprecipitation assays were performed as in **(B)** using protein extracts from 8-d-old wild-type and oeDDA1-GFP seedlings. Anti-GFP and anti-CUL4 antibodies were used to detect DDA1-GFP and CUL4, respectively. Immunoblots against RPT5 were used as a loading control.

representative. The results showed that the protein–protein interaction rate for DDA1 and PYL8 was of the same magnitude as that of DDA1 with DDB1a (Figure 4D). Finally, in agreement with yeast two-hybrid data, no interaction was found for any other component of the CDD complex and PYL8 in BiFC assays (Supplemental Figure 5).

The PYL8 ABA Receptor Is Ubiquitinated and Degraded by the Proteasome

The CDD complex has been shown to facilitate ubiquitination and subsequent degradation of specific protein targets by the ubiquitin-proteasome system (UPS) (Osterlund et al., 2000; Chen et al., 2006; Castells et al., 2010). The fact that PYL4, PYL8, and PYL9 interact with DDA1, a component of the CDD, opens the possibility that they are substrates of the UPS. To test this possibility, we focused our analysis on PYL8, since it has been shown that, among functionally redundant PYR/PYL/RCAR proteins, PYL8 has a significant role in mediating ABA signaling (Antoni et al., 2013). Thus, we first assessed whether PYL8 is degraded at the 26S proteasome by treating *Arabidopsis* seedlings expressing a 3xHA-tagged PYL8 fusion (oe3HA-PYL8) (Antoni et al., 2013) with the proteasome inhibitor MG132. Immunoblots using anti-HA antibodies showed increased 3HA-PYL8 protein accumulation in MG132-treated samples compared with mock controls (Figure 5A). Moreover, upon proteasome inhibition, several high molecular mass bands were detected, likely corresponding to ubiquitinated 3HA-PYL8 forms. To confirm PYL8 ubiquitination, Ub-conjugated proteins were purified from oe3HA-PYL8 plants using commercially available p62 resin that has an affinity for Ub and binds it noncovalently. Immunoblots using anti-HA antibodies showed the precipitation of 3HA-PYL8 as multiple high molecular mass bands when samples were incubated with p62 resin but not when the empty resin was used, indicating that 3HA-PYL8 is modified by polyubiquitin chains in planta (Figures 5B and 5C).

DDA1 Overexpression Promotes PYL8 Protein Degradation

Because PYL8 is targeted for degradation by the proteasome and DDA1 and PYL8 physically interact, we investigated whether DDA1 mediates PYL8 destabilization. For this, we compared the rate of degradation of 3HA-PYL8 with that in plants that overexpress both DDA1-GFP and 3HA-PYL8 (obtained by crossing between oe3HA-PYL8 and oeDDA1-GFP line 3; Figure 3A). These assays were performed in the presence of the protein synthesis inhibitor cycloheximide (CHX), precluding any effect due to variation in transgene expression between samples over time. As a result, we found that DDA1-GFP overexpression increased 3HA-PYL8 degradation after 60 min compared with oe3HA-PYL8 controls (Figures 5D and 5E; Supplemental Figure 6). Interestingly, ABA treatments limited 3HA-PYL8 degradation, although this effect was reduced when DDA1-GFP was overexpressed (Figures 5D and 5E). qRT-PCR analysis corroborated that none of these effects was caused by changes in the expression of the *3HA-PYL8* transgene (Supplemental Figure 7A). In these experiments, treatment of plants from both genotypes with the proteasome inhibitor MG132 attenuated 3HA-PYL8 destabilization, further confirming proteasomal regulation of PYL8 stability (Figure 5F).

It has been shown previously that PYR/PYL/RCAR ABA receptors accumulate in seeds where they mediate ABA inhibition of seed germination (Gonzalez-Guzman et al., 2012). Thus, we tested whether DDA1 also regulates PYL8 levels in seeds. Immunoblots of protein extracts from imbibed seeds showed that DDA1-GFP overexpression decreases 3HA-PYL8 accumulation in both ABA-treated and nontreated seeds (Figures 5G and 5H; Supplemental Figure 8A). Again, ABA led to increased accumulation of 3HA-PYL8. qRT-PCR analysis indicated that changes in 3HA-PYL8 levels did not correlated with variations in the expression of the corresponding transgene (Supplemental Figure 7B). Taken together, these results indicate that DDA1 and ABA play opposite roles in the regulation of PYL8 accumulation: whereas DDA1 facilitates PYL8 degradation, ABA prevents its destabilization.

ABA Limits PYL8 Polyubiquitination

To characterize the mechanism of action of ABA on PYL8 stabilization, we first tested whether ABA impairs the interaction of

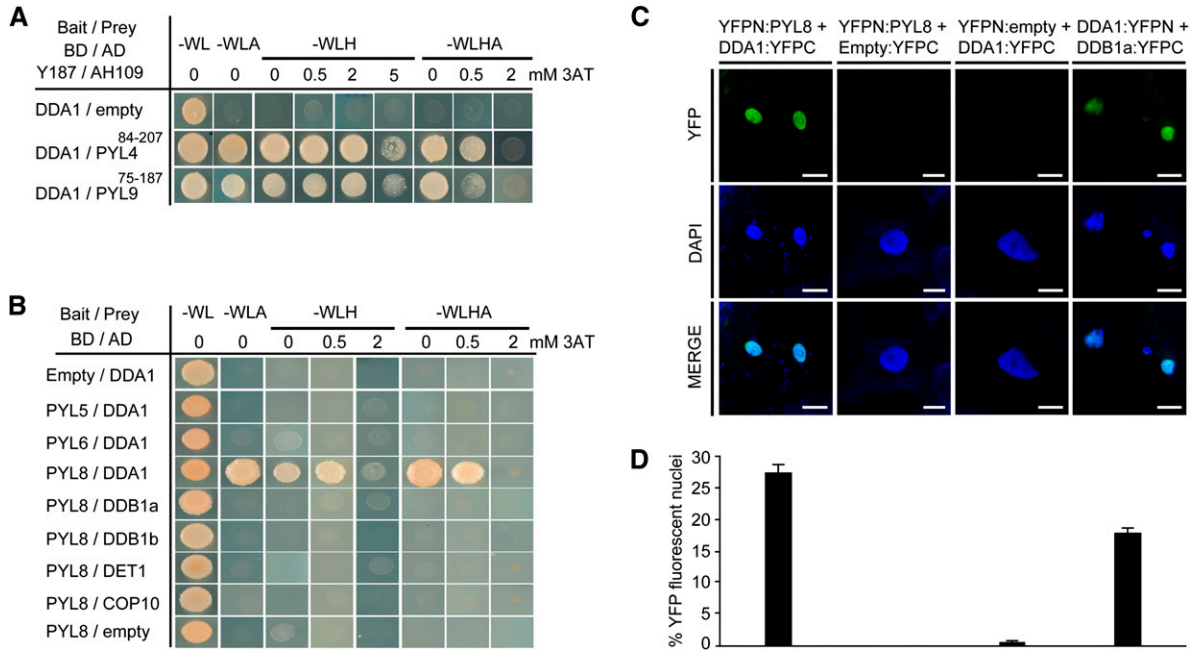

Figure 4. DDA1 Interacts with Members of the PYR/PYL/RCAR Family of ABA Receptors.

(A) Y187 yeast cells transformed with pGBKT7-DDA1 were used to screen a cDNA library prepared from *Arabidopsis* seedlings in the pGADT7 vector and transformed into AH109 cells. Positive clones included truncated versions of the ABA receptors PYL4 and PYL9. Yeast clones were grown in selective media containing different concentrations of 3-amino-1,2,4-triazole (3AT; ranging from 0.5 to 5 mM). Empty pGADT7 vector was used as a negative control.

(B) DDA1 interaction with full-length PYL5, PYL6, and PYL8 was assessed using yeast two-hybrid experiments. The physical association between PYL8 and other components of the CDD complex (DDB1a, DDB1b, DET1, and COP10) was also tested.

(C) Analysis of DDA1 and PYL8 interaction by BiFC. Confocal images of *N. benthamiana* epidermal cells expressing different construct combinations as indicated were obtained. Reconstitution of YFP fluorescence indicates that the corresponding DDA1 and PYL8 constructs interact directly. DDB1a and DDA1 fusions were used as a positive control. YFP fluorescence, DAPI staining of nuclei, and merged images are shown. Bars = 10 μm.

(D) Percentage of nuclei displaying YFP fluorescence in the BiFC analyses shown in **(C)**. Data represent means and SD for three independent biological replicates; $n > 100$ for each construct combination.

DDA1 and PYL8. For this, both yeast two-hybrid and coimmunoprecipitation assays, using DDA1-GFP and 3HA-PYL8 transiently expressed in *N. benthamiana* leaves, were performed in the presence or absence of ABA. As a result, we found that ABA does not impede DDA1 binding to PYL8 (Figures 6A and 6B). Furthermore, DDA1-GFP coimmunoprecipitated with 3HA-PYL8 only when leaves were treated with ABA, suggesting that PYL8 protection by ABA also helps to stabilize its association to DDA1, which otherwise rapidly promotes PYL8 degradation (Figure 6B). In these assays, we also observed a slight decrease in DDA1-GFP levels upon ABA treatment, pointing to potential ABA regulation of DDA1 accumulation. Indeed, *Arabidopsis* DDA1 seems to be a target itself of the proteasome, as has been shown previously for hDDA1 (Olma et al., 2009) (Figure 6C). However, when we compared the rate of degradation of DDA1-GFP after treatment of plants with CHX, no differences were observed between ABA-treated samples and mock controls (Figure 6D). Next, we checked whether ABA alters the rate of PYL8 polyubiquitination. Toward this, Ub-conjugated proteins were purified after ABA treatment of oe3HA-PYL8 seedlings. Immunoblots showed a marked decrease in 3HA-PYL8 polyubiquitinated bands in ABA-treated leaves compared with mock controls, indicating that ABA inhibits PYL8 polyubiquitination (Figure 6E).

Overexpression of DDA1 Reduces Plant Sensitivity to ABA

Our data indicate that DDA1 facilitates the degradation of PYL8 and likely that of other PYR/PYL/RCAR receptors with which it interacts, pointing to a negative regulatory role for DDA1 in ABA signaling. To test this hypothesis, we characterized several ABA responses in oeDDA1-GFP plants, including ABA-mediated inhibition of seed germination, seedling establishment, and root growth. As a control, we used wild-type and oeHAB1 plants (overexpressing the PP2C phosphatase HAB1; used as an ABA-insensitive control) in these experiments (Saez et al., 2004). Compared with wild-type plants, oeDDA1-GFP plants showed a reduced response to ABA in all cases (Figures 7A to 7C, 7G, and 7H). In addition, oeDDA1-GFP seedlings were less sensitive to NaCl- or mannitol-mediated inhibition of seed germination than the wild type (Figures 7D and 7E), indicating that the DDA1 overexpression effect is also evident under stress conditions that increase endogenous ABA levels (Leung and Giraudat,

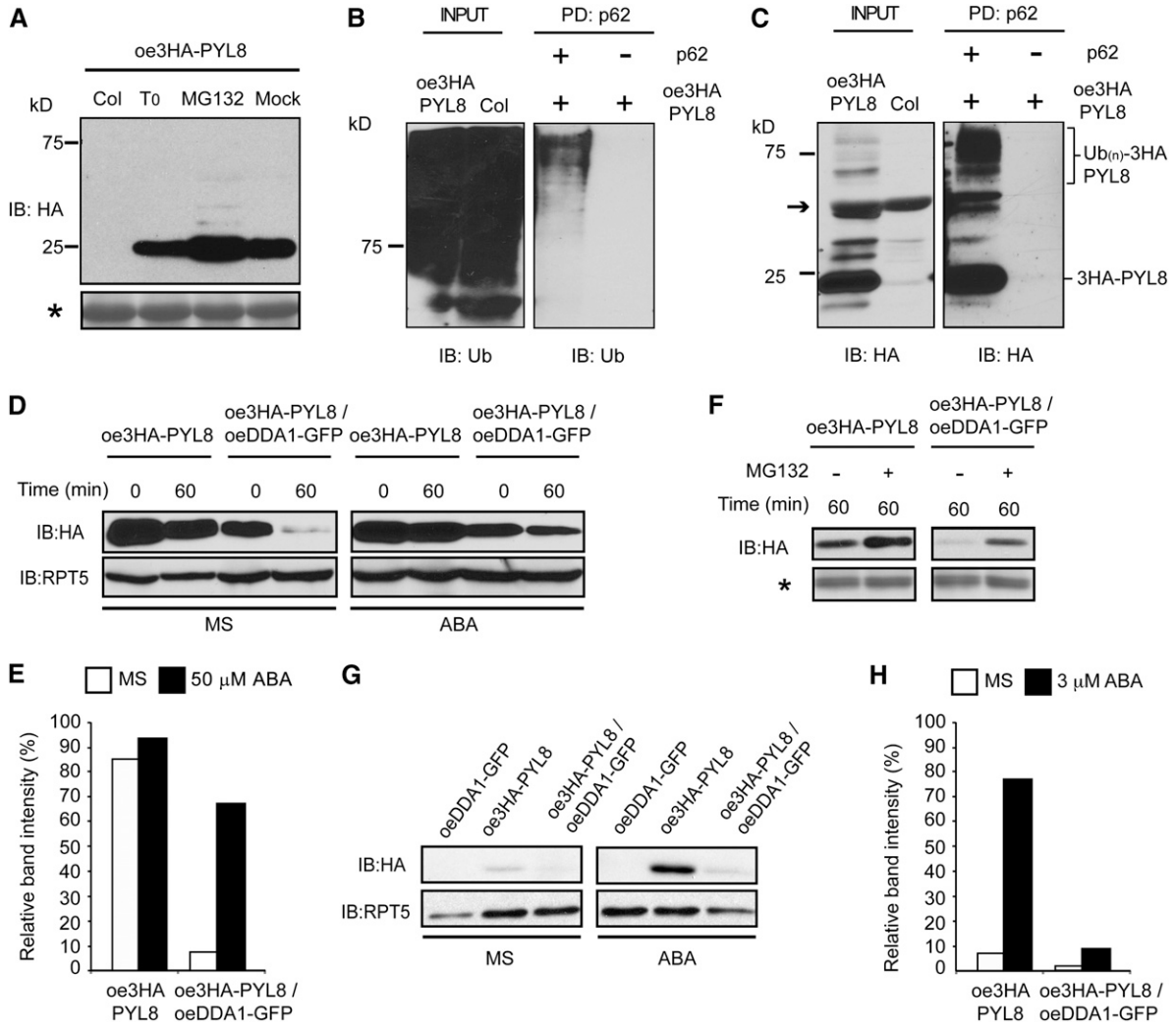

Figure 5. DDA1 Promotes PYL8 Degradation through the Ub Proteasome System.

(A) The proteasome inhibitor MG132 stabilizes 3HA-PYL8. Nine-day-old oe3HA-PYL8 seedlings were treated or not (Mock) during 2 h with 50 μM MG132. Plant extracts from time 0 (T_0) were used as a control. The panel labeled with an asterisk (also in **[F]**) shows Ponceau staining of Rubisco as a loading control.

(B) and **(C)** Affinity purification of polyubiquitinated 3HA-PYL8. oe3HA-PYL8 protein extracts were incubated with Ub binding p62 resin or with empty agarose resin (negative control). Anti-Ub antibody was used in **(B)** to detect total ubiquitinated proteins. Anti-HA allowed the detection of 3HA-PYL8 and its ubiquitinated forms [$Ub_{(n)}$-3HA-PYL8; indicated by the bracket] in **(C)**. Wild-type (Col) protein extracts were used as immunoblot controls. The arrow indicates the position of a nonspecific protein detected by anti-HA.

(D) Immunoblot analyses of 3HA-PYL8 levels (detected using anti-HA antibody) in 8-d-old oe3HA-PYL8/oeDDA1-GFP and control (oe3HA-PYL8) seedlings treated with 50 μM CHX for 60 min in the presence (ABA) or absence of 50 μM ABA. Both lines were in the *pyl8-1* background. Anti-RPT5 antibody was used for loading control purposes.

(E) Protein level analysis of samples described in **(D)** was performed using ImageJ software. Protein levels at 60 min are shown relative to the initial values (time 0; 100%) for each genotype and treatment.

(F) Immunoblots showing 3HA-PYL8 stabilization by the proteasome inhibitor MG132 in CHX-treated plants.

(G) Immunoblot analysis of 3HA-PYL8 levels in seeds of the genotypes described in **(D)**. Prior to protein extraction, imbibed seeds were maintained for 24 h in MS medium with or without 3 μM ABA. Immunoblot conditions were as in **(D)**.

(H) Protein level analysis in the seed samples described in **(G)** was performed using ImageJ software.

Immunoblot analyses shown in **(D)** and **(G)** were repeated at least three times with similar results (Supplemental Figures 6 and 8).

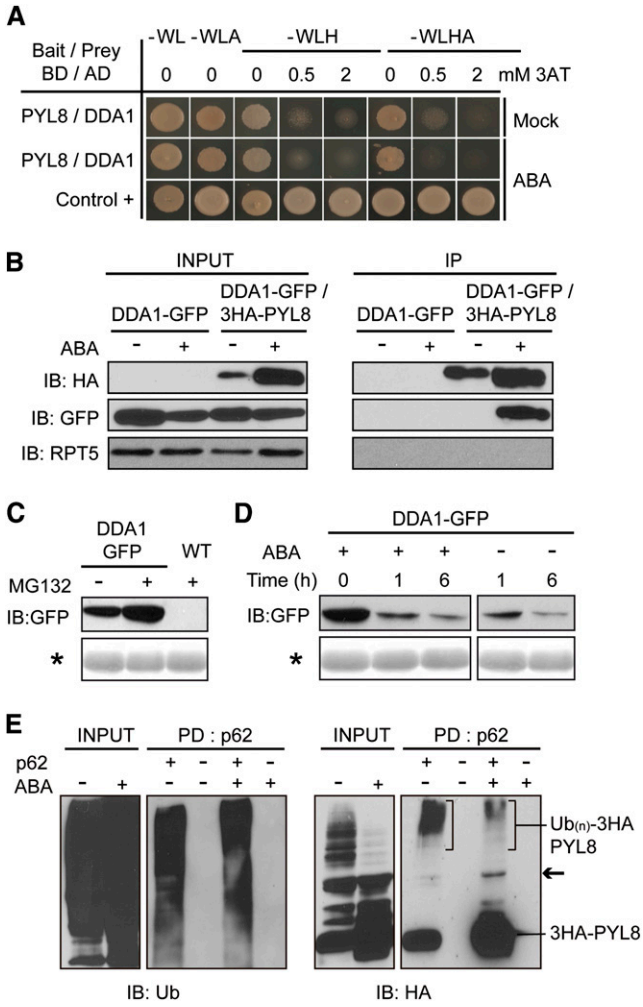

Figure 6. ABA Reduces PYL8 Polyubiquitination but Not Its Interaction with DDA1.

(A) ABA does not disrupt PYL8 and DDA1 interaction in yeast two-hybrid assays. Yeast transformed with the indicated constructs were grown on selective plates with 100 mM ABA and compared with mock controls. Selective media contained different concentrations of 3-amino-1,2,4-triazole (3AT; ranging from 0.5 to 2 mM). pGAD-T and pGBK-53 clones (Clontech) were used as the positive control (Control +).

(B) DDA1-GFP associates with 3HA-PYL8 in the presence of ABA in vivo. 3HA-PYL8 and DDA1-GFP fusions were transiently expressed in 3-week-old *N. benthamiana* leaves treated with MG132 in the presence or absence of 50 μM ABA. Total extracts (INPUT) and immunoprecipitates (IP) were subjected to immunoblot analysis with anti-GFP and anti-FLAG antibodies. Anti-RPT5 antibody was used for loading control purposes.

(C) Immunoblot showing DDA1-GFP stabilization by the proteasome inhibitor MG132. Nine-day-old DDA1-GFP seedlings were treated or not for 2 h with 50 μM MG132. DDA1-GFP was detected using anti-GFP antibody. Wild-type plant extracts were used as an immunoblot negative control. The panel labeled with an asterisk (also in **[D]**) shows Ponceau staining of Rubisco as a loading control.

(D) Time course of the relative abundance of DDA1-GFP in 9-d-old seedlings treated with 50 μM CHX in the presence or absence of 50 μM ABA.

(E) ABA treatments reduce 3HA-PYL8 polyubiquitination. For affinity purification of polyubiquitinated 3HA-PYL8, total protein extracts obtained from oe3HA-PYL8 seedlings treated or not with ABA were incubated with Ub binding p62 resin or with empty agarose resin (negative control). Anti-Ub antibody was used to detect total ubiquitinated proteins. Anti-HA antibody allowed the detection of 3HA-PYL8 and its ubiquitinated forms [$Ub_{(n)}$-3HA-PYL8; indicated by the brackets]. The arrow indicates the position of a nonspecific protein detected by anti-HA.

1998; Seo and Koshiba, 2002). For these experiments, we used ABA-hyposensitive *coi1-16 resistant to ABA1* (*cra1*) mutants as a control (Fernandez-Arbaizar et al., 2012).

To confirm that reduced sensitivity to ABA is due to DDA1 overexpression, we obtained *Arabidopsis* plants expressing the cDNA of *DDA1* under the control of a β-estradiol–inducible promoter (iDDA1). Seed establishment rates of iDDA1 plants grown in Murashige and Skoog (MS) medium supplemented or not with ABA or with β-estradiol were indistinguishable from those of wild-type plants. However, the establishment rate increased in iDDA1 seedlings compared with the wild type upon induction of DDA1 expression (i.e., when both ABA and β-estradiol were added to the medium) (Figures 7F and 7I).

Reduced CDD Function Causes ABA Hypersensitivity

In order to functionally characterize DDA1 in plants, we searched for loss-of-function mutants in different *Arabidopsis* T-DNA insertion collections. All available lines contained the T-DNA integrated into noncoding regions in the *DDA1* gene and displayed transcript levels similar to those of wild-type plants, which precluded their use in further studies. Similar results were found when *DDA1* gene silencing approaches were followed, as all *Arabidopsis* transgenic lines obtained using two different RNA interference systems (Karimi et al., 2002; Hilson et al., 2004) displayed normal *DDA1* mRNA levels. As an alternative, we sought to characterize mutants of other CDD components, since DDA1 forms part of the CDD complex. As expected, analysis of ABA responses showed that mutations that yield reduced function of DDB1, DET1, or COP10 (note that their total loss of function is lethal) (Schroeder et al., 2002; Suzuki et al., 2002; Bernhardt et al., 2010) caused an opposite ABA phenotype to that of DDA1-overexpressing plants. Thus, *ddb1a*, *cop10-4*, and *det1-1* mutants showed an increased response to ABA-mediated inhibition of germination and seedling establishment compared with wild-type plants (Figures 8A to 8C). In the case of *det1-1* mutants, ABA hypersensitivity also extended to root growth responses (Figures 8D and 8E).

Next, we determined whether ABA hypersensitivity correlates with increased accumulation of PYL8 in plants showing reduced CDD function. For this analysis, we used *cop10-4* mutants as a representative of CDD-deficient mutants. Immunoblots of protein extracts obtained from imbibed seeds showed that *cop10-4* mutation increases 3HA-PYL8 accumulation in both ABA-treated and nontreated seeds (Figures 8F and 8G; Supplemental Figure 8B). qRT-PCR analysis indicated that changes in 3HA-PYL8 levels did not correlate with variations in the expression of the corresponding transgene (Supplemental Figure 7C). Altogether, these results suggest that cooperation between CDD components exists to regulate ABA receptor stability and, therefore, to modulate ABA responses.

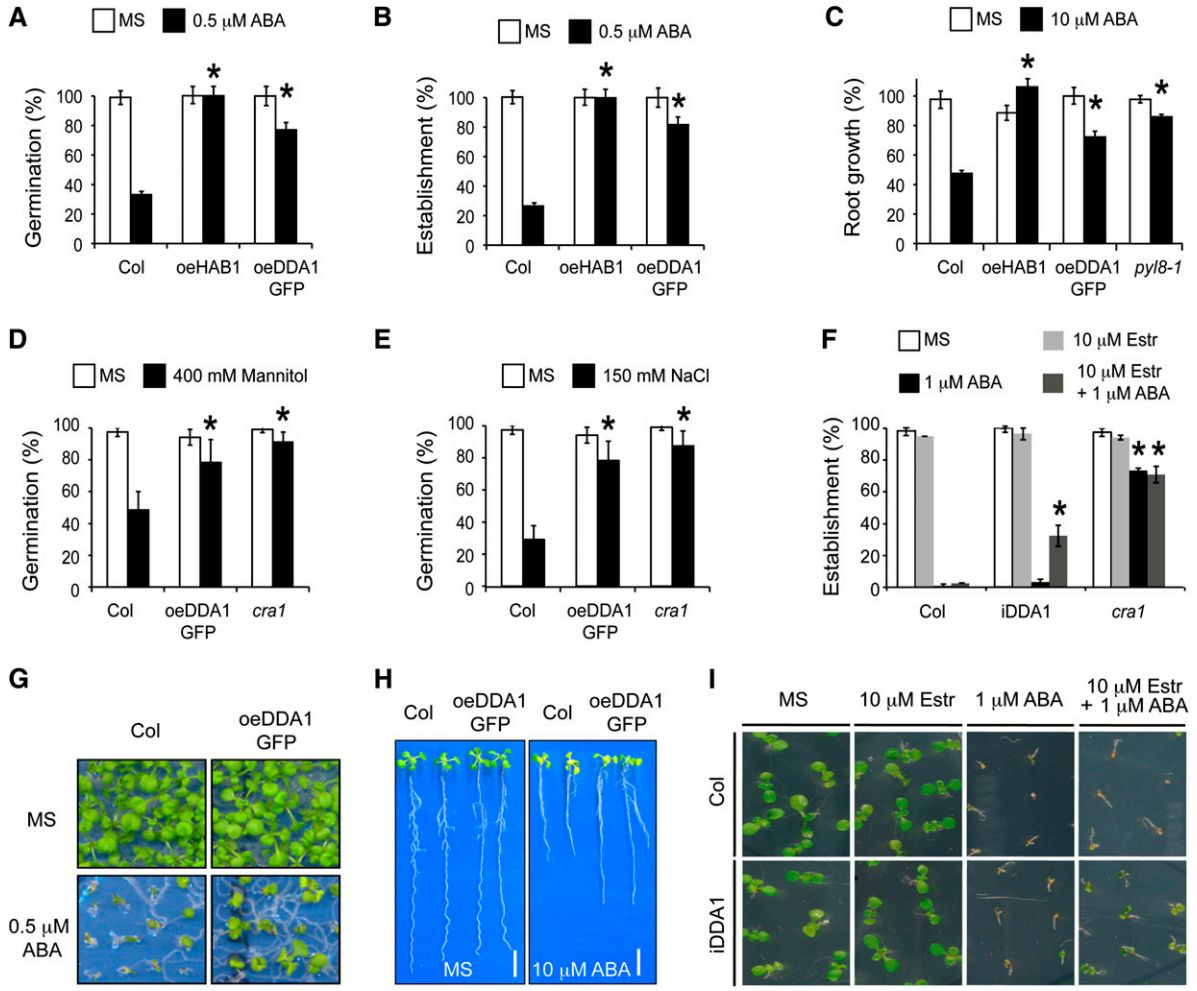

Figure 7. DDA1-Overexpressing Plants Show Reduced Sensitivity to ABA.

(A) The percentage of seeds that germinated (radicle emergence) in the presence of 0.5 μM ABA at 72 h after sowing was compared with wild-type (Col), oeDDA1-GFP, and oeHAB1 (ABA-insensitive control) lines.

(B) Percentage of seeds that germinated and developed green cotyledons and the first pair of true leaves at 5 d. The same genotypes as in **(A)** were compared.

(C) Quantification of ABA-mediated root growth inhibition. The same genotypes as in **(A)** were compared together with *pyl8-1* mutants.

(D) and **(E)** The percentage of seeds that germinated in the presence of 400 mM mannitol **(D)** or 150 mM NaCl **(E)** at 5 d after sowing was analyzed in wild-type and oeDDA1-GFP plants. ABA-insensitive *cra1* mutants were used as a control.

(F) Percentage of seeds that germinated and developed green cotyledons at 5 d in the presence or not of 1 μM ABA and/or 10 μM β-estradiol (Estr). Genotypes corresponded to wild-type plants, *cra1* mutants, and plants expressing *DDA1* under the control of a β-estradiol–inducible promoter (iDDA1).

(G) ABA-mediated growth inhibition of wild-type and oeDDA1-GFP seedlings that were germinated on 0.5 μM ABA as in **(B)**. Photographs were taken 10 d after sowing.

(H) Reduced sensitivity to ABA-mediated inhibition of root growth from oeDDA1-GFP plants compared with the wild type analyzed as in **(C)**. Bars = 1 cm.

(I) Photographs of plants analyzed in **(F)** taken 10 d after sowing.

*$P < 0.01$ (Student's *t* test) with respect to the wild type in the same experimental conditions. In all cases, data are means of three biological replicates. Error bars represent SD. MS medium (MS) was used as a control in all assays.

DISCUSSION

CDD complexes have been proposed to play a dual role in regulating CRL4 activity by enhancing the E3 activity of CRL4, likely through its COP10 subunit, and facilitating CRL4 target recognition (Yanagawa et al., 2004; Pick et al., 2007; Olma et al., 2009). In the latter case, it has been suggested that CDD complexes may act as adaptor modules for additional substrate receptors (Lau and Deng, 2012). Our results on the biochemical and functional characterization of *Arabidopsis* DDA1 strongly support this model. Thus, we found

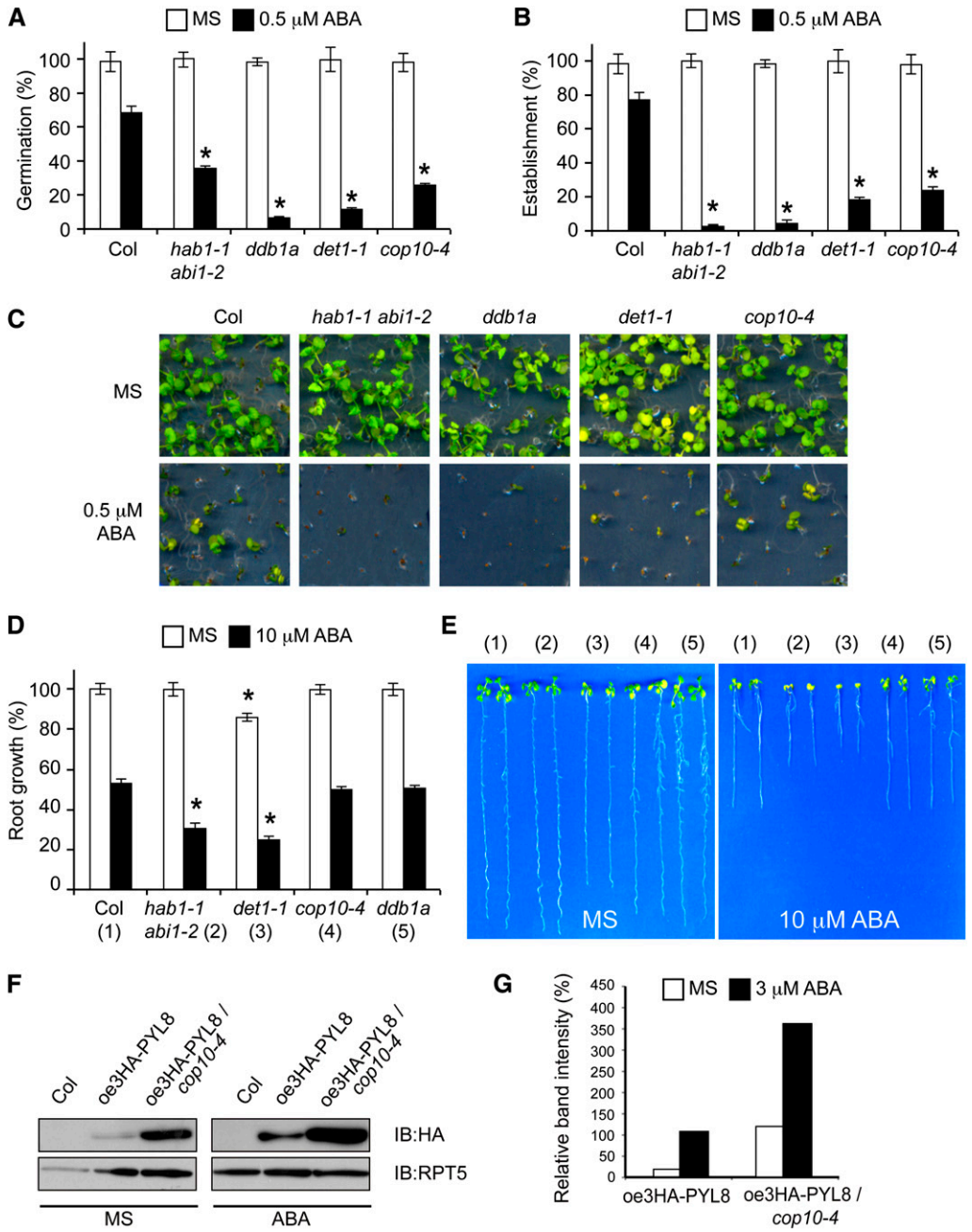

Figure 8. Mutants in CDD Complex Components Show Enhanced Sensitivity to ABA.

(A) Comparison of the percentage of seeds that germinated (radicle emergence) in the presence of 0.5 μM ABA at 4 d after sowing for wild-type (Col), *hab1-1 abi1-2*, *det1-1*, *cop10-4*, and *ddb1a* plants.

(B) Percentage of seeds that germinated and developed green cotyledons and the first pair of true leaves at 7 d. Genotypes analyzed were as in **(A)**.

(C) Photographs of representative seedlings taken 10 d after sowing.

(D) Quantification of ABA-mediated root growth inhibition of the wild type (1) compared with *hab1-1 abi1-2* (2), *det1-1* (3), *cop10-4* (4), and *ddb1a* (5) mutants. Seeds were germinated on MS medium and transferred to 10 μM ABA for 10 d.

(E) Photographs of representative seedlings analyzed in **(D)** taken 10 d after transferring seedlings to plates lacking or containing 10 μM ABA.

(F) Immunoblot analysis of 3HA-PYL8 levels in seeds corresponding to the *pyl8-1* (oe3HA-PYL8) and *cop10-4*/*pyl8-1* (oe3HA-PYL8/*cop10-4*) backgrounds. Prior to protein extraction, imbibed seeds were maintained for 24 h in MS medium with or without 3 μM ABA. Anti-HA and anti-RPT5 antibodies were used to detect 3HA-PYL8 and for loading control purposes, respectively. Analyses were repeated at least three times with similar results (Supplemental Figure 8).

(G) Protein-level analysis of samples described in **(F)** was performed using ImageJ software.

*$P < 0.01$ (Student's *t* test) with respect to the wild type in the same experimental conditions. Data shown in **(A)**, **(B)**, and **(D)** are means of three biological replicates. Error bars represent SD.

that DDA1 associates with the CDD complex and CUL4 in vivo and is involved in direct protein target recognition for ubiquitination and subsequent degradation by the proteasome. The association of DDA1 with plant CDD complexes has been suggested previously (Chen et al., 2010). Here, we demonstrate that DDA1 is a component of CDD using two approaches. First, we were able to detect DDA1 in biochemically purified CDD fractions. CDD purification yielded partially degraded COP10 and DET1 products, as seems to be the case for DDA1 too, which might have precluded its identification in the study by Yanagawa et al. (2004). Second, we found all CDD components in TAP-purified DDA1 samples. Similar to its human counterpart, DDA1 association with CDD, and therefore CRL4, is mediated by its interaction with the BPA domain in DDB1 proteins (Jin et al., 2006; Pick et al., 2007).

The biochemical activity of DDA1 has been a matter of discussion since its identification in mammalian systems (Pick et al., 2007; Olma et al., 2009; Chen et al., 2010). One hypothesis was that DDA1 might play a structural role as part of CDD/DDD-E2 complexes. However, DDA1 is apparently not required to maintain the integrity of these complexes, since the CDD complex could be reconstituted in vitro in the absence of DDA1 (Chen et al., 2006). Another possibility was that DDA1 might be necessary to activate certain CRL4s by stabilizing the DDB1 association with a specific subset of DCAFs. Indeed, immunoprecipitation assays showed that both endogenous and tagged hDDA1 associate with DDB1, CUL4, and several DCAF proteins, including COP1, AMBRA, and Cockayne syndrome A in human cells (Jin et al., 2006; Olma et al., 2009; Behrends et al., 2010). However, experimental evidence showing DDA1-mediated stabilization of DDB1-DCAF complexes has not been provided. In this study, we propose a different function for DDA1 as a substrate receptor for CRL4 Ub ligases. In this regard, we identified a target of DDA1 activity, the ABA receptor PYL8. Despite functional redundancy between PYR/PYL/RCAR ABA receptors, PYL8 has a prominent role in mediating ABA signaling at the roots (Antoni et al., 2013). Consistent with the DDA1 regulation of PYL8 function, oeDDA1-GFP plants demonstrated reduced sensitivity to ABA-mediated inhibition of root growth, as is also the case for *pyl8-1* mutants. Notably, DDA1 overexpression also altered responses that are regulated by highly redundant PYR/PYL/RCAR family members, including seed germination and seedling establishment (Gonzalez-Guzman et al., 2012), suggesting a broader role for DDA1 in regulating ABA receptor stability. In agreement with this, we found that DDA1 also interacts in vivo with PYL4 and PYL9, which may represent additional targets for DDA1. However, we did not observe an interaction of DDA1 with PYL5 and PYL6 in yeast two-hybrid assays, suggesting that a certain degree of specificity in DDA1 activity may exist. DDA1 function toward ABA receptors is very likely performed in the context of the CDD, as indicated by the increased sensitivity to ABA of mutants of other members of the complex. Accordingly, *cop10-4* plants accumulated higher levels of PYL8 protein than wild-type plants, as it is expected for plants with reduced DDA1 function. However, no other CDD component was able to interact with PYL8 under our experimental conditions, highlighting the specificity and preponderance of DDA1 in ABA receptor recognition. These results are consistent with a model in which the whole CDD complex acts as a substrate adaptor module for CRL4 where DDA1 mediates the recognition of specific targets (Figure 9).

It is noteworthy that ABA and DDA1 play opposite roles in the regulation of PYL8 stability, where ABA and DDA1 prevent and promote PYL8 degradation, respectively. Since ABA signaling is obviously strongly dependent on the activity of PYR/PYL/RCAR receptors, an ABA-dependent protection mechanism for receptor stability would serve to reinforce and sustain ABA signaling, particularly during the early stages of signaling. However, at later stages, plant desensitization to ABA likely occurs in order to prevent the adverse effects of continuous ABA responses (i.e., growth reduction or stomatal closure). Accordingly, it has been shown that ABA reduces *PYL8* gene expression after 3 h of treatment (Saavedra et al., 2010). Interestingly, ABA treatment of oeHA-PYL8 seeds for 24 h also reduced *HA-PYL8* transcript levels (Supplemental Figure 7), suggesting posttranscriptional regulation of *PYL8* mRNA by ABA. Our results on DDA1 further emphasize the complexity and sophistication of the regulatory network that modulates ABA signaling. Thus, DDA1-mediated degradation of ABA receptors should also contribute to desensitizing the pathway when stress conditions disappear and ABA levels diminish. This regulatory mechanism might also be instrumental to impairing ABA signaling during germination, since it has been shown that ABA concentration in seeds is reduced upon imbibition (Figure 9).

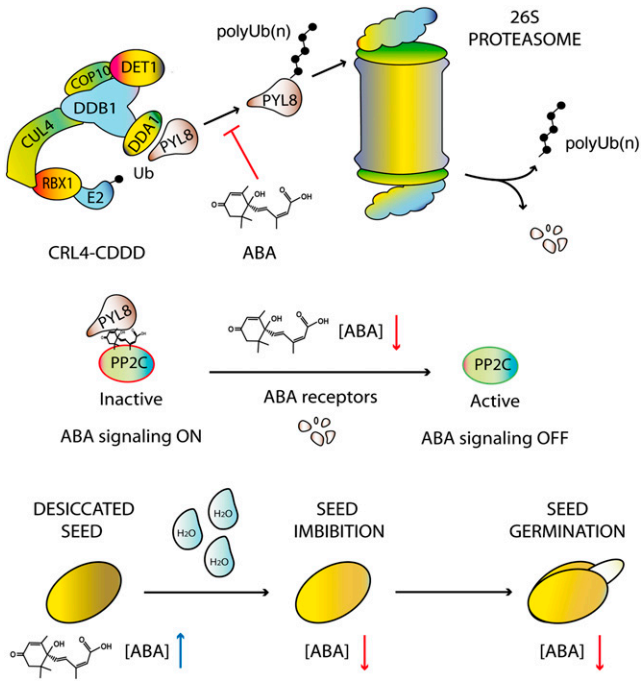

Figure 9. Model for DDA1's Role in ABA Desensitization.

DDA1, as part of the CDDD (COP10-DET1-DDB1-DDA1) substrate adaptor module, allows the recognition and ubiquitination of ABA receptors (e.g., PYL8) by CRL4 Ub ligases. Polyubiquitinated ABA receptors are then degraded at the 26S proteasome. ABA, on the contrary, stabilizes the receptors by limiting their polyubiquitination (top panel). Low ABA levels enable DDA1-mediated destabilization of ABA receptors, favoring the release and activation of PP2C phosphatases, which act as negative regulators of ABA signaling (middle panel). In this way, DDA1 contributes to ABA desensitization when levels for this hormone diminish (i.e., when stress conditions disappear or during seed imbibition and germination) (bottom panel).

The molecular aspects underlying ABA-mediated protection of PYL8 remain unknown. This mechanism apparently does not imply disruption of the PYL8–DDA1 interaction or a reduction of DDA1 levels but rather a decrease in PYL8 polyubiquitination rates. One possibility is that changes in receptor conformation driven by ABA binding limit PYL8 ubiquitination. Thus, it is known that PYL8 interacts in an ABA-dependent manner at least with five clade A PP2Cs in vivo (Saavedra et al., 2010; Antoni et al., 2013). The ternary complex PP2C-ABA-PYL8 shows high stability (K_d around 20 to 40 nM), and the interaction of PYL8 with ABA and PP2C generates substantial changes in receptor conformation (Melcher et al., 2009; Santiago et al., 2009). Therefore, it is possible that the formation of such complexes may hide specific Lys residues on PYL8 and thereby interfere with its polyubiquitination. Further biochemical and molecular studies should help us to unveil the precise details of such a protective mechanism. Definition of the structural details of DDA1 binding to specific PYR/PYL/RCAR proteins in the presence of CDD and CRL4 complexes, and/or PP2Cs and ABA, will also help to elucidate how DDA1 substrate specificity is attained (note that DDA1 lacks the WDxR motifs usually required for substrate interaction) and to better understand the modulation of ABA signaling based on the regulation of ABA receptor stability.

Previous reports have highlighted the relevance of the UPS in the regulation of ABA responses by identifying E3 Ub ligases whose alteration leads to changes in plant sensitivity to ABA (reviewed in Antoni et al., 2011; Lyzenga and Stone, 2012; Guo et al., 2013). These belong to different E3 types and, according to their effects, can be categorized as positive or negative regulators of plant responses to ABA. Thus, several RING-type E3 ligases, such as ABA-INSENSITIVE RING PROTEIN1, SALT AND DROUGHT INDUCED RING FINGER1, XERICO, RING-H2 E3 LIGASE2a (RHA2a), and RHA2b, act as positive regulators of ABA signaling (Ko et al., 2006; Zhang et al., 2007; Bu et al., 2009; Ryu et al., 2010; Li et al., 2011). Accordingly, loss-of-function mutants for these RING-type E3s are insensitive to ABA, whereas overexpressing transgenic lines display ABA hypersensitivity. On the other hand, DROUGHT TOLERANCE REPRESSOR (DOR), also belonging to the RING type, N-recognin PROTEOLYSIS6, and DWD HYPERSENSITIVE TO ABA PROTEINS3 (DWA3) negatively regulate ABA responses, including ABA-driven stomatal closure (i.e., DOR) or ABA-mediated inhibition of seed germination and root growth (Zhang et al., 2008a; Holman et al., 2009; Lee et al., 2011). Despite the important role of these E3s in the modulation of ABA responses, the identities of their protein targets remain unknown. Indeed, the identified UPS targets within the ABA signaling pathways are almost restricted to key transcription factors regulating the expression of ABA-responsive genes. This is the case of the B3-type transcription factor ABI3 (targeted by the RING-type ABI3-INTERACTING PROTEIN2; Zhang et al., 2005), HD-ZIP ATHB6 (targeted by $CUL3^{MATH-BTB}$ E3 ligases; Lechner et al., 2011), and the ABA-responsive transcription factors ABI4 (Finkelstein et al., 2011), ABF2 (targeted by the BTB protein ARIA; Kim et al., 2004), ABF3 (Sirichandra et al., 2010), and bZIP ABI5. Interestingly, in line with the notion that tight regulation of ABI5 levels is required to modulate ABA responses (Lopez-Molina et al., 2001), two different E3 ligases promote ABI5 ubiquitination and degradation at the proteasome. Thus, KEEP ON GOING and DWA1/DWA2 E3s are known to modulate ABI5 protein levels (Stone et al., 2006; Lee et al., 2010; Liu and Stone, 2010). The latter are canonical WDxR motif–containing DCAF proteins that provide target specificity to CRL4 complexes, in this case toward ABI5, a transcription factor that acts downstream in the ABA signaling pathway (Lee et al., 2008). Our results unveil a regulatory role for CRL4 complexes, mediated by DDA1, at the initial stage of ABA signaling, where they affect ABA receptor function. In this way, our study provides further evidence about the versatility of CRL4 E3 ligases and strengthens the importance of the UPS in the regulation of plant responses to ABA.

METHODS

Plant Materials and Growth Conditions

Arabidopsis thaliana plants used in this study, including mutants and transgenic plants, were of the Columbia-0 ecotype. Plants were grown in MS medium (Murashige and Skoog, 1962) with 1% Suc at 21°C under a 16-h-light/8-h-dark cycle using cool-white fluorescent light conditions (100 mmol m^{-2} s^{-1}). Specific treatments were performed as stated in each experiment (see below and figure legends). Mutants *cop10-4*, *det1-1*, *cra1*, *hab1-1 abi1-2*, and *pyl8-1* and transgenic lines oe3HA-PYL8, FLAG-COP10, and oeHAB1 have been described previously (Peeper et al., 1994; Suzuki et al., 2002; Yanagawa et al., 2004; Fernandez-Arbaizar et al., 2012; Antoni et al., 2013). The T-DNA insertion line corresponding to *ddb1a* was obtained from TAIR (http://www.arabidopsis.org; SALK_038757). To generate transgenic plants expressing DDA1, the *DDA1* cDNA was amplified using Expand High Fidelity polymerase (Roche) and the Gateway-compatible primers DDA1-BF (5′-GGGGACCACTTTGTACAAGAAAGCTGGGTAGAATAGTGAGCAACTTTAAGTCGA-3′) and DDA1-BR (5′-GGGGACCACTTTGTACAAGAAAGCTGGGTATAAGCCCTGAGTAGATGAAGAAGAAGACG-3′). PCR products were cloned into the pDONR207 plasmid (Invitrogen) by in vitro recombination using Gateway BP reaction kits (Invitrogen) and verified by Sanger sequencing. Then, DDA1 cDNA was transferred, using Gateway LR reaction kits (Invitrogen) to pGWB5 (Nakagawa et al., 2007) and pMDC7 (Curtis and Grossniklaus, 2003) destination vectors. The resulting plasmids were used to generate oeDDA1-GFP and iDDA1 lines, respectively. In all cases, plant transformation was performed by transferring the corresponding constructs to *Agrobacterium tumefaciens* C58C1 (pGV2260) competent cells (Deblaere et al., 1985). Transformation of *Arabidopsis* plants was performed by the floral dip method (Clough and Bent, 1998). T1 transgenic seeds were selected based on corresponding selection markers, and T3 homozygous progeny were used for further studies. Lines oeDDA1-GFP/oeFLAG-COP10, oe3HA-PYL8/*pyl8-1*/oeDDA1-GFP, and oe3HA-PYL8/*pyl8-1*/*cop10-4* were generated by crossing the corresponding homozygous parental lines. F2 segregating progeny of these crosses were selected in the corresponding antibiotics to isolate homozygous plants for each construct.

For BiFC and coimmunoprecipitation experiments, *Nicotiana benthamiana* plants were grown in soil in the greenhouse at 22°C under a 16-h-light/8-h-dark photoperiod prior to agroinfiltration of leaves with the corresponding constructs.

qRT-PCR

To analyze *DDA1-GFP* expression, qRT-PCR experiments were performed using RNA extracted from Columbia-0 wild-type and oeDDA1-GFP plants. Three biological replicates, consisting of tissue pooled from 15 to 20 plants from different plates, were taken. RNA extraction and cleanup were done with the RNeasy mini kit (Qiagen) and DNase digestion to remove genomic DNA contamination. cDNA was synthesized from 1 μg of total RNA using a high-capacity cDNA reverse transcription kit (Applied Biosystems).

Ten microliters from one-tenth-diluted cDNA was used to amplify *DDA1* and the housekeeping gene *ACTIN8* using FastStart Universal Probe Master (Roche). The primers used were DDA1-RTF (5′-CCCTCCGATCCTTC-TAATCC-3′), DDA1-RTR (5′-GCTGCGTATAAGAATGTTTTTCAC-3′), ACT8-F (5′-GGTACTGGAATGGTTAAGGC-3′), and ACT8-R (5′-GTCCAACACAA-TACCGGTTG-3′).

qRT-PCR experiments for the analysis of *3HA-PYL8* levels in seedlings were performed as mentioned above. In the case of seeds, RNA extraction was performed as described previously (Oñate-Sánchez and Vicente-Carbajosa, 2008). cDNA was synthetized using the Transcriptor first-strand cDNA synthesis kit (Roche). The cDNA reaction was diluted 1:10 in water, and 10 μL was used for qRT-PCR analysis with the primers HA-F (5′-CTATGACGTCCCGGACTATGCA-3′) and PYL8-R (5′-CACTGATTATCCACAAGCTCA-3′). The FastStart Universal SYBR Green Master mix (Roche) was used for amplification with the *ELONGATION FACTOR1*α (*EF1*α) gene as an internal control (EF1α-F, 5′-CCCAGGCTGATTGTGCTGT-3′, and EF1α-R, 5′-GGGTG-GTGGCATCCATCTTGTT-3′).

Quantitative PCR was performed on 96-well optical plates in a 7300 Real Time PCR system (Applied Biosystems). The PCR conditions were as follows: 2 min at 50°C, 10 min at 95°C, and 40 cycles of 15 s at 95°C and 30 s at 60°C.

TAP Assays

Cloning of a GS-TAP–tagged DDA1 fusion under the control of the constitutive cauliflower mosaic virus 35S promoter and transformation of *Arabidopsis* cell suspension cultures were performed as described previously (Van Leene et al., 2007). TAP of protein complexes was done using the GS tag (Burckstummer et al., 2006) followed by protein precipitation and separation, according to Van Leene et al. (2008). For the protocols of proteolysis and peptide isolation, acquisition of mass spectra by a 4800 MALDI TOF/TOF Proteomics Analyzer (AB SCIEX), and mass spectrometry–based protein homology identification based on the TAIR genomic database, we referred to Van Leene et al. (2010). Experimental background proteins were subtracted based on ~40 TAP experiments on wild-type cultures and cultures expressing TAP-tagged mock proteins GUS, RFP, and GFP (Van Leene et al., 2010).

Yeast Two-Hybrid Experiments

The full-length *DDA1* cDNA was cloned into pGBKT7 (Gal4 DNA binding domain; Clontech). This construct was used to screen a whole seedling cDNA library (Bustos et al., 2010) prepared in the pGADT7 vector (Gal4 activation domain; Clontech) to detect DDA1-interacting proteins.

To confirm protein interactions, plasmids were cotransformed into *Saccharomyces cerevisiae* AH109 cells following standard heat-shock protocols (Chini et al., 2007). Successfully transformed colonies were identified on yeast synthetic dropout medium lacking Leu and Trp; these colonies were resuspended in water and transferred to selective medium lacking Ade, His, Leu, and Trp. Plates without His were supplemented with different concentrations of 3-amino-1,2,4-triazole (ranging from 0.5 to 10 mM). Yeast cells were incubated at 30°C for 6 d. Empty vectors were cotransformed as negative controls.

To test the DDA1 interaction with specific DDB1a domains, DDB1a truncated versions were generated and cloned into the pGADT7 vector as follows: BPA (amino acids 16 to 350), BPB (amino acids 387 to 704), BPA + BPB (amino acids 16 to 704), BPC (amino acids 704 to 1002), and BPB + BPC (amino acids 350 to 1002). Full-length DDB1a was used as a positive control. To check whether the DDA1–PYL8 interaction is altered by ABA, yeast cotransformed with pGAD-PYL8 and pGBK-DDA1 constructs were grown in selective medium (as described above) supplemented with 100 mM ABA or an equal volume of solvent (ethanol) as a mock control.

BiFC Experiments

Different combinations of *Agrobacterium* clones expressing fusion proteins as indicated were coinfiltrated into the abaxial surface of 3-week-old *N. benthamiana* plants as described (Voinnet et al., 2003). The p19 protein was used to suppress gene silencing. The empty vectors were used as negative controls. Fluorescence was visualized in epidermal cells of leaves after 3 d of infiltration using a Leica sp5 confocal microscope. Nuclei were visualized after submerging the leaves in a DAPI solution (1 μg/mL DAPI in 100 mM phosphate buffer and 0.5% Triton X-100).

For counting YFP fluorescent nuclei, images of *N. benthamiana* leaf areas, agroinfiltrated with different construct combinations, were analyzed using ImageJ software. To count YFP nuclei in a consistent manner, the epifluorescence image contrast setting was adjusted to the same values for all samples. Total nuclei counts were obtained from confocal microscopy images of the same areas showing DAPI-stained nuclei (blue channel). A minimum of 100 nuclei were counted for each construct combination in each biological replicate.

Protein Extraction, Coimmunoprecipitation Assays, and Immunoblots

For protein extraction from seedlings, proteins were extracted in buffer containing 50 mM Tris-HCl, pH 7.4, 150 mM NaCl, 10 mM $MgCl_2$, 1 mM phenylmethylsulfonyl fluoride, 0.1% Nonidet P-40 and 1× complete protease inhibitor (Roche). After centrifugation at 16,000*g* at 4°C, the supernatants were collected. This step was repeated twice. For protein extraction from seeds, seeds were frozen in liquid N_2 and then homogenized in buffer containing 7 M urea, 2 M thiourea, 4% (w/v) 3-[(3-cholamidopropyl)dimethylammonio]-1-propanesulfonate, 18 mM Tris-HCl, pH 7.5, 0.2% Triton X-100, and 1× complete protease inhibitor (Roche). After 10 min of incubation at 4°C with rotation, DTT was added to protein extracts (14 mM final concentration) prior to 20 min of incubation at 4°C. Extracts were clarified by centrifugation as mentioned above. Protein concentration in the final supernatants was determined using the Bio-Rad Protein Assay kit.

For coimmunoprecipitation assays in *Arabidopsis*, normalized seedling protein extracts were incubated with 5 μL of anti-GFP antibody (Living Colors Full-Length A.V. polyclonal antibody; Clontech) for 1 h at 4°C with rotation. Twenty microliters of protein A–coupled beads (prewashed twice with 0.1 M Gly, pH 2.7) was added to the samples and incubated for an additional 1 h at 4°C with rotation. After washing three times with 500 μL of extraction buffer, samples were denatured, separated on SDS-PAGE gels, and transferred onto polyvinylidene difluoride membranes (Millipore). For coimmunoprecipitation assays in *N. benthamiana*, 3-week-old leaves were infiltrated with the indicated constructs and, after 3 d, treated with 50 μM ABA for 24 h. Protein extracts were incubated with Anti-HA Affility Matrix (Roche) for 4 h at 4°C with rotation. After washing three times with 500 μL of extraction buffer, samples were separated on SDS-PAGE gels and transferred as described above.

For immunoblots, membranes were probed with different antibodies: anti-GFP-HRP at 1:2000 dilution (for DDA1-GFP detection; Milteny Biotec), monoclonal anti-FLAG M2 at 1:1000 dilution (for FLAG-COP10; Sigma-Aldrich), anti-CUL4 at 1:500 dilution (Chen et al., 2006), anti-DET1 at 1:1000 dilution, and anti-DDB1 at 1:2000 dilution (Zhang et al., 2008b). For immunodetection of 3HA-PYL8, anti-HA-HRP (Roche) was used at 1:1000 dilution. To confirm equal protein loading, membranes were stained with Ponceau reagent or immunoblotted using anti-RPT5 at 1:1000 dilution (Kwok et al., 1999).

The CDD complex was purified as described previously (Yanagawa et al., 2004). For the analysis of purified CDD complex fractions, proteins in each fraction were separated onto 15% SDS-PAGE gels. Silver staining and immunoblotting using anti-DDA1 antibodies were performed to visualize specific protein bands. For anti-DDA1 production, see below.

Purification of Recombinant Proteins and Antibody Production

Recombinant His-DDA1 protein was expressed in the *Escherichia coli* BL21 (DE3) strain carrying a pET28-HisT7DDA1 construct. Bacteria were cultured in Luria-Bertani medium at 37°C to an OD at 600 nm of 0.6, at which time protein expression was induced with 0.2 mM isopropyl-D-thiogalactopyranoside for 3 h. Cell lysis was performed using a French press, and lysates were clarified by centrifugation at 16,000*g* for 30 min at 4°C. His-DDA1 protein was purified from lysates with nickel–nitrilotriacetic acid agarose beads under denaturing conditions (Qiagen) and eluted with a pH gradient as described by the manufacturer. Protein concentration in the final eluates was determined using the Bio-Rad Protein Assay kit. To raise anti-DDA1 antibodies, purified His-DDA1 protein was introduced into two rabbits (1 mg/each). Rabbit preimmune serum was kept to check for anti-DDA1 specificity.

Affinity Purification of Ubiquitinated Proteins

Isolation of ubiquitinated proteins was performed as described previously (Manzano et al., 2008) with small modifications. Briefly, proteins were extracted from oe3HA-PYL8 plants treated with 50 μM MG132 using buffer BI (50 mM Tris-HCl, pH 7.5, 20 mM NaCl, 0.1% Nonidet P-40, and 5 mM ATP) plus plant protease inhibitor cocktail (Sigma-Aldrich), 1 mM of phenylmethylsulfonyl fluoride, 50 μM MG132, 10 nM Ub aldehyde, and 10 mM *N*-ethylmaleimide. Protein extracts were incubated with 40 μL of prewashed p62 agarose (Wilkinson et al., 2001) or the agarose alone at 4°C for 4 h. Afterward, the beads were washed two times with 1 mL of BI buffer and once more with 1 mL of BII buffer (BI plus 200 mM NaCl) and proteins were eluted by boiling in 50 μL of SDS loading buffer. The eluted proteins were separated by SDS-PAGE and analyzed by immunoblotting using anti-Ub antibody (Boston Biochem) to detect the presence of ubiquitinated proteins or anti-HA-HRP antibody (Roche) for 3HA-PYL8 detection. To test the effect of ABA, leaves were treated for 24 h with 50 μM ABA or an equal volume of solvent (ethanol) as a mock control.

In Vivo Protein Degradation Assays

Seedlings were grown in MS solid medium for 8 d and then transferred to liquid MS medium containing 50 μM CHX (Sigma-Aldrich) in the presence or absence of 50 μM ABA (Sigma-Aldrich). The effect of proteasome inhibition was tested by adding 50 μM MG132 (Sigma-Aldrich) to the liquid MS medium. Whole plant samples were harvested at specific time points as indicated. Protein extraction and immunoblotting were performed as mentioned above. ImageJ version 1.37 software (http://rsb.info.nih.gov/ij) was used to analyze protein band intensity.

Seed Germination and Seedling Establishment Assays

After surface sterilization of the seeds, stratification was conducted in the dark at 4°C for 3 d. Next, ~100 seeds of each genotype were sown on MS plates lacking or supplemented with 0.5 μM ABA, 150 mM NaCl, or 400 mM mannitol. In the analyses of iDDA1 lines, 1 μM ABA was used and β-estradiol was added to medium at 10 μM final concentration as stated. To score seed germination, radicle emergence was analyzed at 72 and 96 h after sowing. Seedling establishment was scored after 5 d as the percentage of seeds that developed green expanded cotyledons and the first pair of true leaves.

Root Growth Assays

Seedlings were grown on vertically oriented MS plates for 4 to 5 d. Afterward, 20 plants were transferred to new MS plates lacking or supplemented with 10 μM ABA. The plates were scanned on a flatbed scanner after 10 d to produce image files suitable for quantitative analysis of root growth using ImageJ version 1.37 software.

Phylogenetic Analysis

DDA1 homologs were searched in different databases, Plaza (http://bioinformatics.psb.ugent.be/plaza/), Phytozome (http://www.phytozome.net), Gramene (http://www.gramene.org), TAIR (http://www.arabidopsis.org), and GenBank (http://www.ncbi.nlm.nih.gov), using web-hosted BLAST applications (http://blast.ncbi.nlm.nih.gov/Blast.cgi). All truncated DDA1 sequences were excluded in subsequent analyses. Sequences were aligned using ClustalW2 (http://www.ebi.ac.uk/Tools/msa/clustalw2/) with the Gonnet protein comparison matrix and default parameters (gap opening penalty of 10 and gap extension penalty of 0.1 for initial pairwise alignment; gap opening penalty of 10 and gap extension penalty of 0.2 for the multiple alignment; with residue-specific and hydrophilic residue penalties, a gap separation distance of 4 and a 30% delay divergent cutoff) and then manually inspected to check for possible misalignments (Supplemental Data Set 1). The best model fitting the alignment was selected using ProtTest (Abascal et al., 2005), which corresponded to a Jones-Taylor-Thornton model for amino acid substitution with a discrete gamma distribution (four categories), a proportion of invariant, and an initial BIONJ tree. This model was used to conduct a maximum likelihood analysis with bootstrapping using 1000 replicates using the MEGA 5 (http://www.megasoftware.net/) software. The gaps/missing treatment parameter was set to complete deletion. The more distant homologs, from *Selaginella moellendorffii* and *Picea glauca*, were used as an outgroup to root the resulting phylogenetic tree.

Accession Numbers

Sequence data from this article can be found in the Arabidopsis Genome Initiative database under the following accession numbers: *DDA1* (At5g41560), *DDB1A* (At4g05420), *DDB1B* (At4g21100), *COP10* (At3g13550), *DET1* (At4g10180), *CUL4* (At5g46210), *PYL8* (At5g53160), *PYL4* (At2g38310), and *PYL9* (At1g01360).

Supplemental Data

The following materials are available in the online version of this article.

Supplemental Figure 1. Multiple Sequence Alignment of Plant DDA1 Proteins Obtained Using ClustalW2 Software.

Supplemental Figure 2. Maximum-Likelihood Phylogenetic Tree of Plant DDA1 Proteins.

Supplemental Figure 3. DDA1 Detection in Purified CDD Fractions.

Supplemental Figure 4. DDA1 Binds the ABA Receptors PYL4 and PYL9 in Vivo.

Supplemental Figure 5. DDA1, but Not Other CDDD Complex Components, Binds the ABA Receptor PYL8 in Vivo.

Supplemental Figure 6. DDA1 and ABA Play Opposite Roles in the Regulation of PYL8 Accumulation.

Supplemental Figure 7. Analysis of *3HA-PYL8* Expression Levels in in Vivo Degradation and Seed Samples.

Supplemental Figure 8. DDA1 and COP10 Regulate PYL8 Accumulation in Seeds.

Supplemental Table 1. Protein Identification Details Obtained with the 4800 MALDI TOF/TOF Proteomics Analyzer and the GPS Explorer Version 3.6 Software Package Combined with the Search Engine Mascot Version 2.2.

Supplemental Data Set 1. Multiple Sequence Alignment of Plant DDA1 Proteins in FASTA Format.

ACKNOWLEDGMENTS

We thank Oscar Lorenzo for providing *cra1* mutant seeds, Haodong Chen for the anti-CUL4 antibody, Tsuyoshi Nakagawa and Sumie Ishiguro for providing pGWB Gateway vectors, Mark Curtis and Ueli Grossniklaus for pMDC7 plasmid, and the Nottingham Arabidopsis Stock Centre and ABRC for supplying mutant lines and cDNAs. We thank Salomé Prat, Maite Sanmartín, Michael Sauer, Carlos Alonso-Blanco, Enrique Rojo, and Roberto Solano for helpful discussion on the manuscript. We also thank José Ramón Valverde for help in phylogenetic analyses. This research was supported by the Spanish Ministry of Economy and Competitiveness (MINECO; National Research Program, Grants BIO2010-18820 to V.R., BIO2011-29085 to J.P.-A., and BIO2011-23446 to P.L.R.; INNPACTO Program, Grant IPT-310000-2010-9 to J.P.-A.; and CONSOLIDER Program, Grant 2007-28317 to J.P.-A.), the National Science Foundation (Grant GM-47850 to X.W.D.), and the National Institutes of Health (Grant GM-47850 to X.W.D.). E.I. and L.R. were recipients of Formación de Personal Investigador fellowships from MINECO.

AUTHOR CONTRIBUTIONS

M.L.I., E.I., P.L.R., X.W.D., and V.R. conceived the study and designed the experiments. M.L.I., E.I., L.R., M.I.P., Y.Y., E.P., E.S., G.D.J., and V.R. generated lines and constructs and performed the experiments. M.L.I., E.I., N.W., J.P.-A., G.D.J., P.L.R., X.W.D., and V.R. analyzed the data. V.R. wrote the article. All authors revised the article.

Received December 20, 2013; revised December 20, 2013; accepted February 5, 2014; published February 21, 2014.

REFERENCES

Abascal, F., Zardoya, R., and Posada, D. (2005). ProtTest: Selection of best-fit models of protein evolution. Bioinformatics **21:** 2104–2105.

Antoni, R., Gonzalez-Guzman, M., Rodriguez, L., Peirats-Llobet, M., Pizzio, G.A., Fernandez, M.A., De Winne, N., De Jaeger, G., Dietrich, D., Bennett, M.J., and Rodriguez, P.L. (2013). PYRABACTIN RESISTANCE1-LIKE8 plays an important role for the regulation of abscisic acid signaling in root. Plant Physiol. **161:** 931–941.

Antoni, R., Rodriguez, L., Gonzalez-Guzman, M., Pizzio, G.A., and Rodriguez, P.L. (2011). News on ABA transport, protein degradation, and ABFs/WRKYs in ABA signaling. Curr. Opin. Plant Biol. **14:** 547–553.

Behrends, C., Sowa, M.E., Gygi, S.P., and Harper, J.W. (2010). Network organization of the human autophagy system. Nature **466:** 68–76.

Bernhardt, A., Mooney, S., and Hellmann, H. (2010). Arabidopsis DDB1a and DDB1b are critical for embryo development. Planta **232:** 555–566.

Biedermann, S., and Hellmann, H. (2011). WD40 and CUL4-based E3 ligases: Lubricating all aspects of life. Trends Plant Sci. **16:** 38–46.

Bu, Q., Li, H., Zhao, Q., Jiang, H., Zhai, Q., Zhang, J., Wu, X., Sun, J., Xie, Q., Wang, D., and Li, C. (2009). The Arabidopsis RING finger E3 ligase RHA2a is a novel positive regulator of abscisic acid signaling during seed germination and early seedling development. Plant Physiol. **150:** 463–481.

Bürckstümmer, T., Bennett, K.L., Preradovic, A., Schütze, G., Hantschel, O., Superti-Furga, G., and Bauch, A. (2006). An efficient tandem affinity purification procedure for interaction proteomics in mammalian cells. Nat. Methods **3:** 1013–1019.

Bustos, R., Castrillo, G., Linhares, F., Puga, M.I., Rubio, V., Pérez-Pérez, J., Solano, R., Leyva, A., and Paz-Ares, J. (2010). A central regulatory system largely controls transcriptional activation and repression responses to phosphate starvation in Arabidopsis. PLoS Genet. **6:** e1001102.

Castells, E., Molinier, J., Drevensek, S., Genschik, P., Barneche, F., and Bowler, C. (2010). det1-1-induced UV-C hyposensitivity through UVR3 and PHR1 photolyase gene over-expression. Plant J. **63:** 392–404.

Chen, H., Huang, X., Gusmaroli, G., Terzaghi, W., Lau, O.S., Yanagawa, Y., Zhang, Y., Li, J., Lee, J.H., Zhu, D., and Deng, X.W. (2010). *Arabidopsis* CULLIN4-damaged DNA binding protein 1 interacts with CONSTITUTIVELY PHOTOMORPHOGENIC1-SUPPRESSOR OF PHYA complexes to regulate photomorphogenesis and flowering time. Plant Cell **22:** 108–123.

Chen, H., Shen, Y., Tang, X., Yu, L., Wang, J., Guo, L., Zhang, Y., Zhang, H., Feng, S., Strickland, E., Zheng, N., and Deng, X.W. (2006). *Arabidopsis* CULLIN4 forms an E3 ubiquitin ligase with RBX1 and the CDD complex in mediating light control of development. Plant Cell **18:** 1991–2004.

Chini, A., Fonseca, S., Fernández, G., Adie, B., Chico, J.M., Lorenzo, O., García-Casado, G., López-Vidriero, I., Lozano, F.M., Ponce, M.R., Micol, J.L., and Solano, R. (2007). The JAZ family of repressors is the missing link in jasmonate signalling. Nature **448:** 666–671.

Chinnusamy, V., Gong, Z., and Zhu, J.K. (2008). Abscisic acid-mediated epigenetic processes in plant development and stress responses. J. Integr. Plant Biol. **50:** 1187–1195.

Clough, S.J., and Bent, A.F. (1998). Floral dip: A simplified method for *Agrobacterium*-mediated transformation of *Arabidopsis thaliana*. Plant J. **16:** 735–743.

Curtis, M.D., and Grossniklaus, U. (2003). A Gateway cloning vector set for high-throughput functional analysis of genes in planta. Plant Physiol. **133:** 462–469.

Cutler, S.R., Rodriguez, P.L., Finkelstein, R.R., and Abrams, S.R. (2010). Abscisic acid: Emergence of a core signaling network. Annu. Rev. Plant Biol. **61:** 651–679.

Deblaere, R., Bytebier, B., De Greve, H., Deboeck, F., Schell, J., Van Montagu, M., and Leemans, J. (1985). Efficient octopine Ti plasmid-derived vectors for Agrobacterium-mediated gene transfer to plants. Nucleic Acids Res. **13:** 4777–4788.

Deshaies, R.J., and Joazeiro, C.A. (2009). RING domain E3 ubiquitin ligases. Annu. Rev. Biochem. **78:** 399–434.

Fernández-Arbaizar, A., Regalado, J.J., and Lorenzo, O. (2012). Isolation and characterization of novel mutant loci suppressing the ABA hypersensitivity of the Arabidopsis coronatine insensitive 1-16 (coi1-16) mutant during germination and seedling growth. Plant Cell Physiol. **53:** 53–63.

Finkelstein, R., Lynch, T., Reeves, W., Petitfils, M., and Mostachetti, M. (2011). Accumulation of the transcription factor ABA-insensitive (ABI)4 is tightly regulated post-transcriptionally. J. Exp. Bot. **62:** 3971–3979.

Gonzalez-Guzman, M., Pizzio, G.A., Antoni, R., Vera-Sirera, F., Merilo, E., Bassel, G.W., Fernández, M.A., Holdsworth, M.J., Perez-Amador, M.A., Kollist, H., and Rodriguez, P.L. (2012). *Arabidopsis* PYR/PYL/RCAR receptors play a major role in quantitative regulation of stomatal aperture and transcriptional response to abscisic acid. Plant Cell **24:** 2483–2496.

Guo, L., Nezames, C.D., Sheng, L., Deng, X., and Wei, N. (2013). Cullin-RING ubiquitin ligase family in plant abiotic stress pathways. J. Integr. Plant Biol. **55:** 21–30.

Hauser, F., Waadt, R., and Schroeder, J.I. (2011). Evolution of abscisic acid synthesis and signaling mechanisms. Curr. Biol. **21:** R346–R355.

Hershko, A., and Ciechanover, A. (1998). The ubiquitin system. Annu. Rev. Biochem. **67:** 425–479.

Hilson, P., et al. (2004). Versatile gene-specific sequence tags for Arabidopsis functional genomics: Transcript profiling and reverse genetics applications. Genome Res. **14:** 2176–2189.

Hirayama, T., and Shinozaki, K. (2010). Research on plant abiotic stress responses in the post-genome era: Past, present and future. Plant J. **61:** 1041–1052.

Holman, T.J., et al. (2009). The N-end rule pathway promotes seed germination and establishment through removal of ABA sensitivity in Arabidopsis. Proc. Natl. Acad. Sci. USA **106:** 4549–4554.

Ikeda, F., and Dikic, I. (2008). Atypical ubiquitin chains: New molecular signals. 'Protein Modifications: Beyond the Usual Suspects' review series. EMBO Rep. **9:** 536–542.

Jackson, S., and Xiong, Y. (2009). CRL4s: The CUL4-RING E3 ubiquitin ligases. Trends Biochem. Sci. **34:** 562–570.

Jin, J., Arias, E.E., Chen, J., Harper, J.W., and Walter, J.C. (2006). A family of diverse Cul4-Ddb1-interacting proteins includes Cdt2, which is required for S phase destruction of the replication factor Cdt1. Mol. Cell **23:** 709–721.

Karimi, M., Inzé, D., and Depicker, A. (2002). GATEWAY vectors for Agrobacterium-mediated plant transformation. Trends Plant Sci. **7:** 193–195.

Kim, S., Choi, H.I., Ryu, H.J., Park, J.H., Kim, M.D., and Kim, S.Y. (2004). ARIA, an Arabidopsis arm repeat protein interacting with a transcriptional regulator of abscisic acid-responsive gene expression, is a novel abscisic acid signaling component. Plant Physiol. **136:** 3639–3648.

Ko, J.H., Yang, S.H., and Han, K.H. (2006). Upregulation of an Arabidopsis RING-H2 gene, XERICO, confers drought tolerance through increased abscisic acid biosynthesis. Plant J. **47:** 343–355.

Kwok, S.F., Staub, J.M., and Deng, X.W. (1999). Characterization of two subunits of Arabidopsis 19S proteasome regulatory complex and its possible interaction with the COP9 complex. J. Mol. Biol. **285:** 85–95.

Lau, O.S., and Deng, X.W. (2009). Effect of Arabidopsis COP10 ubiquitin E2 enhancement activity across E2 families and functional conservation among its canonical homologues. Biochem. J. **418:** 683–690.

Lau, O.S., and Deng, X.W. (2012). The photomorphogenic repressors COP1 and DET1: 20 years later. Trends Plant Sci. **17:** 584–593.

Lechner, E., Leonhardt, N., Eisler, H., Parmentier, Y., Alioua, M., Jacquet, H., Leung, J., and Genschik, P. (2011). MATH/BTB CRL3 receptors target the homeodomain-leucine zipper ATHB6 to modulate abscisic acid signaling. Dev. Cell **21:** 1116–1128.

Lee, J.H., Terzaghi, W., and Deng, X.W. (2011). DWA3, an Arabidopsis DWD protein, acts as a negative regulator in ABA signal transduction. Plant Sci. **180:** 352–357.

Lee, J.H., Terzaghi, W., Gusmaroli, G., Charron, J.B., Yoon, H.J., Chen, H., He, Y.J., Xiong, Y., and Deng, X.W. (2008). Characterization of *Arabidopsis* and rice DWD proteins and their roles as substrate receptors for CUL4-RING E3 ubiquitin ligases. Plant Cell **20:** 152–167.

Lee, J.H., Yoon, H.J., Terzaghi, W., Martinez, C., Dai, M., Li, J., Byun, M.O., and Deng, X.W. (2010). DWA1 and DWA2, two *Arabidopsis* DWD protein components of CUL4-based E3 ligases, act together as negative regulators in ABA signal transduction. Plant Cell **22:** 1716–1732.

Leung, J., and Giraudat, J. (1998). Abscisic acid signal transduction. Annu. Rev. Plant Physiol. Plant Mol. Biol. **49:** 199–222.

Li, H., Jiang, H., Bu, Q., Zhao, Q., Sun, J., Xie, Q., and Li, C. (2011). The Arabidopsis RING finger E3 ligase RHA2b acts additively with RHA2a in regulating abscisic acid signaling and drought response. Plant Physiol. **156:** 550–563.

Liu, H., and Stone, S.L. (2010). Abscisic acid increases *Arabidopsis* ABI5 transcription factor levels by promoting KEG E3 ligase self-ubiquitination and proteasomal degradation. Plant Cell **22:** 2630–2641.

Lopez-Molina, L., Mongrand, S., and Chua, N.H. (2001). A postgermination developmental arrest checkpoint is mediated by abscisic acid and requires the ABI5 transcription factor in Arabidopsis. Proc. Natl. Acad. Sci. USA **98:** 4782–4787.

Lyzenga, W.J., and Stone, S.L. (2012). Abiotic stress tolerance mediated by protein ubiquitination. J. Exp. Bot. **63:** 599–616.

Manzano, C., Abraham, Z., López-Torrejón, G., and Del Pozo, J.C. (2008). Identification of ubiquitinated proteins in Arabidopsis. Plant Mol. Biol. **68:** 145–158.

Melcher, K., et al. (2009). A gate-latch-lock mechanism for hormone signalling by abscisic acid receptors. Nature **462:** 602–608.

Murashige, T., and Skoog, F. (1962). A revised medium for rapid growth and bio assays with tobacco tissue cultures. Physiol. Plant. **15:** 473–497.

Nakagawa, T., Kurose, T., Hino, T., Tanaka, K., Kawamukai, M., Niwa, Y., Toyooka, K., Matsuoka, K., Jinbo, T., and Kimura, T. (2007). Development of series of Gateway binary vectors, pGWBs, for realizing efficient construction of fusion genes for plant transformation. J. Biosci. Bioeng. **104:** 34–41.

Nakashima, K., and Yamaguchi-Shinozaki, K. (2013). ABA signaling in stress-response and seed development. Plant Cell Rep. **32:** 959–970.

Olma, M.H., Roy, M., Le Bihan, T., Sumara, I., Maerki, S., Larsen, B., Quadroni, M., Peter, M., Tyers, M., and Pintard, L. (2009). An interaction network of the mammalian COP9 signalosome identifies Dda1 as a core subunit of multiple Cul4-based E3 ligases. J. Cell Sci. **122:** 1035–1044.

Oñate-Sánchez, L., and Vicente-Carbajosa, J. (2008). DNA-free RNA isolation protocols for *Arabidopsis thaliana*, including seeds and siliques. BMC Res. Notes **1:** 93.

Osterlund, M.T., Hardtke, C.S., Wei, N., and Deng, X.W. (2000). Targeted destabilization of HY5 during light-regulated development of Arabidopsis. Nature **405:** 462–466.

Peeper, D.S., van der Eb, A.J., and Zantema, A. (1994). The G1/S cell-cycle checkpoint in eukaryotic cells. Biochim. Biophys. Acta **1198:** 215–230.

Pick, E., Lau, O.S., Tsuge, T., Menon, S., Tong, Y., Dohmae, N., Plafker, S.M., Deng, X.W., and Wei, N. (2007). Mammalian DET1 regulates Cul4A activity and forms stable complexes with E2 ubiquitin-conjugating enzymes. Mol. Cell. Biol. **27:** 4708–4719.

Rubio, S., Rodrigues, A., Saez, A., Dizon, M.B., Galle, A., Kim, T.H., Santiago, J., Flexas, J., Schroeder, J.I., and Rodriguez, P.L. (2009). Triple loss of function of protein phosphatases type 2C leads to partial constitutive response to endogenous abscisic acid. Plant Physiol. **150:** 1345–1355.

Ryu, M.Y., Cho, S.K., and Kim, W.T. (2010). The Arabidopsis C3H2C3-type RING E3 ubiquitin ligase AtAIRP1 is a positive regulator of an abscisic acid-dependent response to drought stress. Plant Physiol. **154:** 1983–1997.

Saavedra, X., Modrego, A., Rodríguez, D., González-García, M.P., Sanz, L., Nicolás, G., and Lorenzo, O. (2010). The nuclear interactor PYL8/RCAR3 of *Fagus sylvatica* FsPP2C1 is a positive regulator of abscisic acid signaling in seeds and stress. Plant Physiol. **152:** 133–150.

Saez, A., Apostolova, N., Gonzalez-Guzman, M., Gonzalez-Garcia, M.P., Nicolas, C., Lorenzo, O., and Rodriguez, P.L. (2004). Gain-of-function and loss-of-function phenotypes of the protein phosphatase 2C HAB1 reveal its role as a negative regulator of abscisic acid signalling. Plant J. **37:** 354–369.

Saez, A., Robert, N., Maktabi, M.H., Schroeder, J.I., Serrano, R., and Rodriguez, P.L. (2006). Enhancement of abscisic acid sensitivity and reduction of water consumption in Arabidopsis by combined inactivation of the protein phosphatases type 2C ABI1 and HAB1. Plant Physiol. **141:** 1389–1399.

Santiago, J., Dupeux, F., Round, A., Antoni, R., Park, S.Y., Jamin, M., Cutler, S.R., Rodriguez, P.L., and Márquez, J.A. (2009). The abscisic acid receptor PYR1 in complex with abscisic acid. Nature **462:** 665–668.

Schroeder, D.F., Gahrtz, M., Maxwell, B.B., Cook, R.K., Kan, J.M., Alonso, J.M., Ecker, J.R., and Chory, J. (2002). De-etiolated 1 and damaged DNA binding protein 1 interact to regulate Arabidopsis photomorphogenesis. Curr. Biol. **12:** 1462–1472.

Seo, M., and Koshiba, T. (2002). Complex regulation of ABA biosynthesis in plants. Trends Plant Sci. **7:** 41–48.

Sirichandra, C., Davanture, M., Turk, B.E., Zivy, M., Valot, B., Leung, J., and Merlot, S. (2010). The Arabidopsis ABA-activated kinase OST1 phosphorylates the bZIP transcription factor ABF3 and creates a 14-3-3 binding site involved in its turnover. PLoS ONE **5:** e13935.

Stone, S.L., Williams, L.A., Farmer, L.M., Vierstra, R.D., and Callis, J. (2006). KEEP ON GOING, a RING E3 ligase essential for *Arabidopsis* growth and development, is involved in abscisic acid signaling. Plant Cell **18:** 3415–3428.

Suzuki, G., Yanagawa, Y., Kwok, S.F., Matsui, M., and Deng, X.W. (2002). Arabidopsis COP10 is a ubiquitin-conjugating enzyme variant that acts together with COP1 and the COP9 signalosome in repressing photomorphogenesis. Genes Dev. **16:** 554–559.

Van Leene, J., Witters, E., Inzé, D., and De Jaeger, G. (2008). Boosting tandem affinity purification of plant protein complexes. Trends Plant Sci. **13:** 517–520.

Van Leene, J., et al. (2007). A tandem affinity purification-based technology platform to study the cell cycle interactome in *Arabidopsis thaliana*. Mol. Cell. Proteomics **6:** 1226–1238.

Van Leene, J., et al. (2010). Targeted interactomics reveals a complex core cell cycle machinery in *Arabidopsis thaliana*. Mol. Syst. Biol. **6:** 397.

Voinnet, O., Rivas, S., Mestre, P., and Baulcombe, D. (2003). An enhanced transient expression system in plants based on suppression of gene silencing by the p19 protein of tomato bushy stunt virus. Plant J. **33:** 949–956.

Wilkinson, C.R., Seeger, M., Hartmann-Petersen, R., Stone, M., Wallace, M., Semple, C., and Gordon, C. (2001). Proteins containing the UBA domain are able to bind to multi-ubiquitin chains. Nat. Cell Biol. **3:** 939–943.

Yanagawa, Y., Sullivan, J.A., Komatsu, S., Gusmaroli, G., Suzuki, G., Yin, J., Ishibashi, T., Saijo, Y., Rubio, V., Kimura, S., Wang, J., and Deng, X.W. (2004). Arabidopsis COP10 forms a complex with DDB1 and DET1 in vivo and enhances the activity of ubiquitin conjugating enzymes. Genes Dev. **18:** 2172–2181.

Yu, J.W., et al. (2008). COP1 and ELF3 control circadian function and photoperiodic flowering by regulating GI stability. Mol. Cell **32:** 617–630.

Zhang, X., Garreton, V., and Chua, N.H. (2005). The AIP2 E3 ligase acts as a novel negative regulator of ABA signaling by promoting ABI3 degradation. Genes Dev. **19:** 1532–1543.

Zhang, Y., Feng, S., Chen, F., Chen, H., Wang, J., McCall, C., Xiong, Y., and Deng, X.W. (2008b). *Arabidopsis* DDB1-CUL4 ASSOCIATED FACTOR1 forms a nuclear E3 ubiquitin ligase with DDB1 and CUL4 that is involved in multiple plant developmental processes. Plant Cell **20:** 1437–1455.

Zhang, Y., Xu, W., Li, Z., Deng, X.W., Wu, W., and Xue, Y. (2008a). F-box protein DOR functions as a novel inhibitory factor for abscisic acid-induced stomatal closure under drought stress in Arabidopsis. Plant Physiol. **148:** 2121–2133.

Zhang, Y., Yang, C., Li, Y., Zheng, N., Chen, H., Zhao, Q., Gao, T., Guo, H., and Xie, Q. (2007). SDIR1 is a RING finger E3 ligase that positively regulates stress-responsive abscisic acid signaling in *Arabidopsis*. Plant Cell **19:** 1912–1929.